



Chemical characteristics of size resolved atmospheric aerosols in Iasi, north-eastern Romania. Nitrogen-containing inorganic compounds controlling aerosols chemistry in the area

5 Alina Giorgiana Galon-Negru¹, Romeo Iulian Olariu^{1,2}, Cecilia Arsene^{1,2}

¹"Alexandru Ioan Cuza" University of Iasi, Faculty of Chemistry, Department of Chemistry, 11 Carol I, 700506 Iasi, Romania

²"Alexandru Ioan Cuza" University of Iasi, Integrated Centre of Environmental Science Studies in the North Eastern Region, 11 Carol I, Iasi 700506, Romania

10 *Correspondence to:* Cecilia Arsene (carsene@uaic.ro); Phone number: +40-232-201354; Fax: +40-232-201313; Postal address: Cecilia Arsene, "Alexandru Ioan Cuza" University of Iasi, Faculty of Chemistry, Department of Chemistry, 11 Carol I, 700506 Iasi, Romania

Abstract. This study assesses the atmospheric aerosol load and behaviour (size and seasonal dependent) of the major inorganic and organic aerosol ionic components (i.e., acetate, ($\text{C}_2\text{H}_3\text{O}_2^-$), formate, (HCO_2^-), fluoride, (F^-), chloride, (Cl^-), nitrite, (NO_2^-), nitrate, (NO_3^-), phosphate, (PO_4^{3-}), sulfate, (SO_4^{2-}), oxalate, ($\text{C}_2\text{O}_4^{2-}$), sodium, (Na^+), potassium, (K^+), ammonium, (NH_4^+), magnesium, (Mg^{2+}) and calcium (Ca^{2+}), in Iasi urban area, north-eastern Romania. Continuous measurements were carried out over 2016 by means of a cascade Dekati Low-Pressure Impactor (DLPI) performing aerosol size classification in 13 specific fractions evenly distributed over the 0.0276 up to 9.94 μm size range. Fine particulate Cl^- , NO_3^- , NH_4^+ and K^+ exhibited clear minima during the warm seasons and clear maxima over the cold seasons, mainly controlled by corroboration between factors such as enhancement in the emission sources, changes in the mixed layer depth and specific meteorological conditions. Fine particulate SO_4^{2-} did not show much variation with respect to seasons. Particulate NH_4^+ and NO_3^- ions were identified as critical parameters controlling aerosols chemistry in the area. The measured concentrations of particulate NH_4^+ and NO_3^- in fine mode ($\text{PM}_{2.5}$) aerosols were found to be in reasonable good agreement with modelled values for winter but not for summer, an observation reflecting actually the susceptibility of NH_4NO_3 aerosols to be lost due to volatility over the warm seasons. Clear evidences have been obtained for the fact that in Iasi, north-eastern Romania, NH_4^+ in $\text{PM}_{2.5}$ is primarily associated with SO_4^{2-} and NO_3^- but not with Cl^- . However, indirect ISORROPIA-II estimations showed that the atmosphere in the investigated area might be ammonia-rich during both the cold and warm seasons, such as enough NH_3 to be present to neutralize H_2SO_4 , HNO_3 and HCl acidic components and to generate fine particulate ammonium salts, in the form of $(\text{NH}_4)_2\text{SO}_4$, NH_4NO_3 and NH_4Cl . ISORROPIA-II runs allowed us estimating that over the warm seasons ~ 35 % of the total analyzed samples presented pH values in the very strong acidity fraction (0–3



pH units range) while over the cold seasons the contribution in this pH range was of ~ 43 %. Moreover, while over the warm seasons ~ 24 – 25 % of the acidic samples were in the 1–2 pH range, reflecting mainly contributions from very strong inorganic acids, over the cold seasons an increase to ~ 40 %, brought by the 1–3 pH range, would reflect possible contributions from other acidic type species (i.e., organics), changes in aerosols acidity impacting most probably the gas–
5 particle partitioning of semi-volatile organic acids. In overall, it has been estimated that within the aerosol mass concentration the ionic mass brings contribution as high as 40.6 % with the rest being unaccounted yet.

Keywords: urban aerosols, ionic chemical composition, ammonium, nitrate, pH, long range transport, Iasi, Romania



1 Introduction

Despite dramatic progress made to improve air quality, at global level air pollution continues to harm people's health and the environment. In Europe and at worldwide level, the aerosols or particulate matter (PM) problem is still of a great concern of interest (Olariu et al., 2015) as Europe and many other areas in the world (e.g., China, India, USA) are some of the most important sources for anthropogenic aerosols.

Atmospheric aerosols, described as complex mixtures of liquid and/or solid particles suspended in a gas (Olariu et al., 2015), are mainly originating from anthropogenic and natural sources (Querol et al., 2004). Fine $PM_{2.5}$ particles (airborne particles with an equivalent aerodynamic diameter $< 2.5 \mu m$) are assigned as air pollutants with significant effects on human health (Pope et al., 2004; Dominici et al., 2006; WHO, 2006a; Directive 2008/50/EC, 2008; Sicard et al., 2011; Ostro et al., 2014), air quality (Directive 2008/50/EC, 2008; Freney et al., 2014), visibility (Tsai and Cheng, 1999; Directive 2008/50/EC, 2008), ecosystems, weather and climate (Ramanathan *et al.*, 2001; Directive 2008/50/EC, 2008; IPCC, 2013) states. However, aerosols are also known to play a significant role within the chemistry of the atmosphere (Prinn, 2003), by providing appropriate surfaces for heterogeneous chemical reactions to occur (Ravishankara, 1997).

Safety threshold values for both the $PM_{2.5}$ (10 or $17 \mu g m^{-3}$ air, as annual mean) and the PM_{10} (airborne particles with an equivalent aerodynamic diameter $< 10 \mu m$; 20 or $28 \mu g m^{-3}$ air, as annual mean) fractions are addressed by the WHO (2006b) or by the 2008/50/EC Directive of the European Parliament and the Council of 21 May 2008 on ambient air quality and cleaner Europe (Directive 2008/50/EC, 2008). With regard to the $PM_{2.5}$ fraction the EEA Report 5 (2015) clearly shows that, for instance, in 2013 the EU daily limit value for PM_{10} was exceeded in 22 out of the 28 EU member states while for the $PM_{2.5}$ the target value was exceeded in 7 states (a decreasing trend is observed when compared with the data in the WHO Report (2006b)). Moreover, it has been recently shown that on a global scale exposure to fine $PM_{2.5}$ leads to about 3.3 million premature deaths per year worldwide (i.e., predominantly in Asia), with an estimate susceptible to double by 2050 (Lelieveld et al., 2015). It was also clearly shown that PM air pollution imparts a tremendous burden to the global public health, ranking it as the 13th leading cause of mortality (Brook, 2008).

Up to now chemical composition of atmospheric aerosols is reported for various urban European sites (Bardouki et al., 2003; Hitzenger et al., 2006; Tursic et al., 2006; Gerasopoulos et al., 2007; Schwarz et al., 2012; Laongsri and Harrison, 2013; Wonaschutz et al., 2015; Sandrini et al., 2016) but at eastern European sites such information is very scarce (Arsene et al., 2011). Sulfate (SO_4^{2-}), nitrate (NO_3^-) and ammonium (NH_4^+) ions are often assigned as significantly contributing inorganic species to the total aerosol mass (Wang et al., 2005; Bressi et al., 2013; Hasheminassab et al., 2014; Voutsas et al., 2014). Ammonium aerosols, with atmospheric lifetime of 1–15 days and clear tendency to deposit at larger distances from their emission sources (Aneja et al., 2000), seem to play a very important role in the atmospheric chemistry. In urban air, fine particulate NO_3^- abundance seems to be mainly controlled by the reaction between HNO_3 and NH_3 (Stockwell et al., 2000), while at a global scale HNO_3 heterogeneous induced reaction on the mineral dust and sea salt particles surface might be the predominant source for particulate NO_3^- (Athanasopoulou et al., 2008; Karydis et al., 2011). In the atmosphere, through



particulate NH_4NO_3 , ammonia currently contributes to effects on human health since there are evidences that this has become gradually more important relative to emissions of oxidized nitrogen (Sutton et al., 2011).

Relative humidity (RH) related reactions (Jang et al., 2002) and gas–particle partitioning processes of semi-volatile species (i.e., ammonia (NH_3), nitric (HNO_3), hydrochloric (HCl) and some organic acids) highly controlled by hydronium ion (H_3O^+) concentrations (Keene et al., 2004; Guo et al., 2016) are responsible on aerosol formation and their chemical composition. Ion balance method (Trebs et al., 2005; Metzger et al., 2006; Arsene et al., 2011), phase partitioning (Meskhidze et al., 2003; Keene et al., 2004) and thermodynamic equilibrium models (e.g., E-AIM, (Clegg et al., 1998; Wexler and Clegg, 2002) or ISORROPIA-II (Nenes et al., 1999; Fountoukis and Nenes, 2007; Hennigan et al., 2015; Guo et al., 2015, 2016; Fang et al., 2017)) often are used to estimate aerosols acidity. Particles acidity might influence transition metals solubility and enhance aerosols toxicity and atmospheric nutrient delivered through atmospheric deposition in marine areas (Meskhidze et al., 2003; Fang et al., 2017).

Apart the scientific progress made in aerosols chemical composition characterization, the aerosols role in the global atmospheric system is not yet sufficiently understood. Aerosols treatment is particularly still very challenging mainly due to the existence of multiple sources (e.g., soil erosion, sea spray, biogenic emission, volcano eruptions, soot from combustion, condensation of precursor gases, and other anthropogenic sources) or due to the complexity of interactions with other atmospheric constituents (Zhang et al., 2015). Nowadays, sources, distribution and behaviour of natural and anthropogenic aerosols are still subjected to much scientific debates even in research groups with a relatively good understanding of the interest matters. However, it is still agreed on the scarcity of aerosols related work for eastern EU countries (EEA Report 5, 2015) but also on the existent discrepancies between theoretically predicted values and those generated from real measurements. The uncertainties are strongly related to secondary inorganic aerosols mainly controlled by the availability of atmospheric sulfuric acid (H_2SO_4), nitric acid (HNO_3) and ammonia (NH_3) (Ianniello et al., 2011). Lack of sufficient detailed observations and emissions data bring high uncertainty in the estimated radiative forcing but it is clearly stated that warming of the climate system is unequivocal, and also that since the 1950s, many of the observed changes are unprecedented (IPCC, 2013).

Despite a growing recognition at international level on the importance related to the air pollution and air quality problems, assessment of the air pollution patterns in Romania remains very scarce. For the north-eastern Romania, there is only limited number of publications mainly concerning the chemical characteristics of the ambient air pollutants (i.e., water soluble ionic constituents of aerosols (Arsene et al., 2011) and rainwater (Arsene et al., 2007)). Recent work performed by Arsene's group in the field of atmospheric chemistry clearly show that in Iasi urban environment (north-eastern Romania), exploring aerosols chemical composition and the chemical processes taking place still involves many unknowns and many challenges (e.g., ~ 59 % of the total aerosol mass concentration unaccounted yet). The present work reports for the first time detailed information concerning the chemical composition and seasonal variation of size segregated water soluble ions in aerosol samples collected for a year in 2016 in Iasi urban area (north-eastern Romania). Consideration is given also on the potential



ongoing chemistry in the area toward the potential contributions brought by critical driving forces as meteorological factors (i.e., relative humidity, temperature), mixed layer depth and emission sources intensity.

2 Experimental

2.1 Measurement site

5 Measurements were performed in Iasi, north-eastern Romania, at the Air Quality Monitoring Station (AMOS, 47°9' N latitude and 27°35' E longitude) of the Integrated Centre of Environmental Science Studies in the North Eastern Region, "Alexandru Ioan Cuza" University of Iasi, CERNESIM-UAIC, Romania. AMOS is located north-east from the city centre, on the rooftop of the highest University building (~ 35 m above the ground level). As AMOS is located in a totally open area the sampling site is assigned as an urban receptor point most probably influenced by well-mixed air masses. A
10 comprehensive demo-geographical characterization of Iasi is described in detail by Arsene et al. (2007, 2011). However, according to a more recent estimate of the Romanian National Institute of Statistics, in 2016 the population in Iasi reached about 362,142 inhabitants (Ichim et al., 2016).

2.2 Field measurements

Size resolved atmospheric aerosols were collected on 25 mm diameter ungreased aluminum filters using a cascade Dekati
15 Low-Pressure Impactor (DLPI) operating at a flow rate of 29.85 L min⁻¹. Similar devices have been successfully used also in other studies (Kocak et al., 2007; Wonaschutz et al., 2015). The DLPI unit performs aerosol size classification in the 0.0276 up to 9.94 µm range using 13 specific fractions evenly distributed (with 0.0276, 0.0556, 0.0945, 0.155, 0.260, 0.381, 0.612, 0.946, 1.60, 2.39, 3.99, 6.58, 9.94 µm at 50 % calibrated aerodynamic cut-point diameters). Sampling performance of the DLPI unit was verified through comparison with simultaneous measurements performed with the stacked filter unit (SFU)
20 system previously used by Arsene et al. (2011). During sampling neither denuders nor backup-filters were used which would mean that sampling artifacts of semi-volatile species (e.g., NH₄NO₃ and NH₄Cl) cannot be completely excluded. Before each reuse the sampler's components were cleaned with ultra pure water and methanol. Disposable polyethylene gloves were always used to avoid hand contact with sampling components. The sampler's components were assembled and disassembled in a Labguard Class II Safety Biological Cabinet, NuAire, disposed in one of CERNESIM's location. The DLPI sampler was
25 transported to and from the field in tightened polyethylene bags.

Sampling was performed over the entire 2016 time period, twice a week, on weekend and working days. A total of 84 sampling events (41 during the cold seasons covering October to March time-interval, and 43 during the warm seasons covering April to September time-interval), generating 1092 size resolved aerosol samples, were collected and analyzed over the entire period. Sampling was carried out on a 36 h basis, with each sampling event starting at 18:00 local time. A volume
30 of 64.33 ± 0.85 m³ (given as an average of the 84 sampling events) was collected per each 36-hour based event. At least two field blanks (consisting of loaded sampler taken to and from the field but never removed from its tightened polyethylene



bag) were generated and simultaneously analyzed with the laboratory blanks in order to determine either or not contamination occurred during the sampler loading, transport, or analysis.

Meteorological parameters including atmospheric temperature (AT), relative humidity (RH), wind speed (WS), wind direction and global radiation were accessed from the data base available for the Hawk GSM-240 CERNESIM's weather station, running at the AMOS site. Information about the mixed layer depth (the atmospheric boundary layer) and its ability to dilute atmospheric pollutants at the investigated site was obtained from the NOAA Air Resources Laboratory (ARL) website (Stein et al., 2015; Rolph et al., 2017).

2.3 Sample analyses

Aerosols mass for both the $PM_{2.5}$ and PM_{10} fractions was gravimetrically determined using a Sartorius microbalance (MSU2.7S-000-DF, $\pm 0.2 \mu\text{g}$ sensitivity) by weighing aluminium filters before and after sampling. Prior undertaking the weighing procedure, filters stored in Petri dishes were kept for at least 3 days in a conditioned room at a relative humidity (RH) of $40 \pm 2 \%$, and a temperature of $20 \pm 2 \text{ }^\circ\text{C}$. In between different procedure, Petri dishes containing unloaded and loaded filters were appropriately stored in zipped plastic bags.

Chemical analyses for 9 water soluble anions (i.e., acetate, ($\text{C}_2\text{H}_3\text{O}_2^-$), formate, (HCO_2^-), fluoride, (F^-), chloride, (Cl^-), nitrite, (NO_2^-), nitrate, (NO_3^-), phosphate, (PO_4^{3-}), sulfate, (SO_4^{2-}) and oxalate, ($\text{C}_2\text{O}_4^{2-}$)) and 5 water soluble cations (i.e., sodium, (Na^+), potassium, (K^+), ammonium, (NH_4^+), magnesium, (Mg^{2+}) and calcium (Ca^{2+})) were performed by ion chromatography (IC) on a ICS-5000⁺ DP DIONEX ion chromatographic system (Thermo Scientific, SUA). Analyses were performed within a week after sampling, in aqueous extracts of the collected samples. For chemical analysis, steps in the analytical procedures were strictly quality-controlled to avoid any contamination of the samples.

After sampling and all other required preparative steps, one half of each collected filter was ultrasonically extracted for 45 minutes in 5 mL of deionized water (resistivity of $18.2 \text{ M}\Omega\cdot\text{cm}$) produced by a Milli-Q Advantage A10 system (Millipore). Filtered extracts ($0.2 \mu\text{m}$ pore size cellulose acetate filters, ADVANTEC) were analyzed on an IonPac CS12A ($4 \times 250 \text{ mm}$) analytical column for cations and on an IonPac AS22 ($4 \times 250 \text{ mm}$) column for anions, running simultaneously on the DIONEX ICS-5000⁺ DP system. The chromatographic instrumental setup was completed by CSRS $300 \times 4 \text{ mm}$ and AERS $500 \times 4 \text{ mm}$ electrochemical suppressors and conductivity detectors. Ions analyses were performed under isocratic elution mode, using $\text{CO}_3^{2-}/\text{HCO}_3^-$ ($4.5/1.4 \text{ mM}$, 1.2 mL min^{-1}) as mobile phase for anions and methane sulfonic acid (20 mM , 1.0 mL min^{-1}) as mobile phase for cations.

Dionex Seven Anions II and Dionex Six Cations II traceable standard solutions were used to generate calibration curves for each species of interest. Quantitative estimates of the analyzed ions were obtained by interpolation on the constructed linear calibration curves that all had correlation coefficients R^2 well above 0.995. For major analyzed cations and anions, the detection limits (defined as 3 times the standard deviation of blank measurements relative to the methods sensitivity) on a 36 h measurement period were of $0.0003 \mu\text{g m}^{-3}$ for NH_4^+ ($3.2 \mu\text{g L}^{-1}$), $0.001 \mu\text{g m}^{-3}$ for Na^+ ($13.4 \mu\text{g L}^{-1}$), $0.0015 \mu\text{g m}^{-3}$ for K^+ ($19.8 \mu\text{g L}^{-1}$), $0.0002 \mu\text{g m}^{-3}$ for Mg^{2+} ($3.2 \mu\text{g L}^{-1}$), $0.0016 \mu\text{g m}^{-3}$ for Ca^{2+} ($20.6 \mu\text{g L}^{-1}$), $0.0010 \mu\text{g m}^{-3}$ for SO_4^{2-} (13.2



$\mu\text{g L}^{-1}$), $0.0012 \mu\text{g m}^{-3}$ for NO_3^- ($15.1 \mu\text{g L}^{-1}$) and $0.0019 \mu\text{g m}^{-3}$ for Cl^- ($24.9 \mu\text{g L}^{-1}$). Ions concentrations in analyzed blank filters (laboratory and field) were subtracted from their corresponding concentrations in the analyzed aerosol samples. The sum (of detected ions or of the gravimetrically determined mass concentration) over all DLPI stages is termed “PM₁₀ fraction” while the sum over impactor stages from 1 to 10 are termed “PM_{2.5} fraction”. Modal diameters of the size segregated aerosols particles or of the analyzed ionic components (individual or as a sum) were determined by fitting lognormal distributions.

2.4 Estimation of the aerosols acidity

The thermodynamic model proposed by Fountoukis and Nenes (2007), i.e. ISORROPIA-II (<http://isorropia.eas.gatech.edu/>), was used to get an estimate of the in situ potential acidity in the PM_{2.5} fraction in Iasi, north-eastern Romania. ISORROPIA-II thermodynamic equilibrium model calculates the gas/liquid/solid equilibrium partitioning of the K^+ , Ca^{2+} , Mg^{2+} , NH_4^+ , Na^+ , SO_4^{2-} , NO_3^- , Cl^- , aerosol water content and can predict particles pH. Up to now the model has been actually used for various field campaigns data analysis (Nowak et al., 2006; Fountoukis et al., 2009).

To obtain the best predictions of aerosols pH, ISORROPIA-II model was run in the “forward mode” for metastable aerosol state. Preliminary runs of the experimental data in the “reverse mode” did not supplied suitable information. In the “metastable” mode the aerosol is assumed to be present only in the aqueous phase, either supersaturated or not (Fountoukis and Nenes, 2007). As input data into the model, we have used just aerosol-phase ions concentrations measured by the IC, along with relative humidity and temperature data from the Hawk GSM-240 weather station. However, there is suggestion that without accompanying gas-phase data required to constrain the thermodynamic models, a more accurate representation of aerosol pH can be obtained by using the aerosol concentrations as input in “forward mode” calculations (Guo et al., 2015; Hennigan et al., 2015). Under these conditions the model seems to be less sensitive to measurement error than the “reverse mode”. Where required, predicted NH_3 data (as output of ISORROPIA-II thermodynamic equilibrium model) have been used for the interpretation of the results reported in the present work.

2.5 Air mass back trajectories and air mass origin

Air mass back trajectories were calculated using the HYSPLIT 4 model of the NOAA Air Resources Laboratory (Stein et al., 2015; Rolph et al., 2017). 48 h back trajectories, arriving at the investigated site at 18:00 local time (15:00 UTC), were computed at 500, 1000 and 2000 m altitudes above the ground level. Four major sectors of air masses origin were distinguished and their contributions are shown in Fig. 1. The north-eastern (N-E) sector (36.6 %) seems to be the most prevalent while the south-south-eastern (S-SE) sector is the least frequent (11.4 %). The W-SW sector is mainly prevailing during winter, while the N-E sector is most common during summer. North-westerly type sector seems to present a slightly enhanced frequency in winter and summer and, according to James (2007), this would reflect a possible European monsoon circulation. The events from the S-SE sector, prevailing mainly in spring, carried out marine chemical features highly influenced by the Black Sea. Air masses travelling above large (long range transport) or short (local) continental areas,



undertaking faster vertical transport most probably due to the locally/continentally driven buoyancy (Holton, 1979; Seinfeld and Pandis, 1998), were also identified (e.g., in April 2016, 5 sampled events out of the total 8 were highly influenced by fast vertical air masses transport). Quite often, for these events, the air masses from both 500 and 1000 m altitude ceased down in their elevation to below 500 meters (air masses brushing the ground surface) with strong impact on the chemical composition of the collected particles (see also discussion later in the text).

3 Results and discussion

3.1 Variability of PM₁₀ and PM_{2.5} mass concentrations

Table 1 shows summary statistics (median, geometric mean, arithmetic mean, standard deviation, minimum and maximum) for PM₁₀ and PM_{2.5} fractions mass concentrations (gravimetrically determined) at the AMOS site for both working days and weekends. Analyses by statistical tests were applied to determine either or not the differences among the mean of working days (more intense local anthropogenic activities) and weekends are significant. Shapiro-Wilk normality test, applied for both PM_{2.5} ($p = 0.546$, at the 95 % confidence level) and PM₁₀ ($p = 0.682$, at the 95 % confidence level) fractions indicated that the entire data-base sets were normally distributed. Since the difference in the mean values of the two groups was not great enough to reject the possibility that the difference is due to random sampling variability it was assumed that there is not a statistically significant difference between the input groups ($p = 0.987$, at the 95 % confidence level for PM_{2.5} fraction; $p = 0.998$, at the 95 % confidence level for PM₁₀ fraction). Since not statistically significant differences were observed, the result allowed us suggesting that AMOS site is mainly influenced by long range transport rather than local contributions. Moreover, it seems that at this site, the PM₁₀ annual mean mass concentration of $18.95 \mu\text{g m}^{-3}$ do not exceeds the $20 \mu\text{g m}^{-3}$ air annual mean WHO set value, while for the PM_{2.5} fraction the annual mean mass concentration of $16.92 \mu\text{g m}^{-3}$ exceeds the $10 \mu\text{g m}^{-3}$ air annual mean WHO set value (WHO, 2006b).

Table 2 presents the annual and/or seasonal arithmetic means of the PM₁₀ and PM_{2.5} fraction mass concentrations in Iasi, north-eastern Romania, and other various European sites (mean \pm stdev). As seen in Table 2 the annual averages obtained in the present work (i.e., 16.9 ± 9.1 for PM_{2.5} and $18.9 \pm 9.3 \mu\text{g m}^{-3}$ for PM₁₀) are slightly different from those reported by Arsene et al. (2011) (i.e., $10.5 \pm 11.5 \mu\text{g m}^{-3}$ for PM_{1.5} and $38.3 \pm 25.4 \mu\text{g m}^{-3}$ for PM_{>1.5}). Possible explanations for the differences between afore mentioned studies might be seen as results either of different sampling altitudes (35 m in the present work vs. 25 m in Arsene et al. (2011)) or due to an enhanced sampling efficiency of the DLPI unit with regard to fine and ultrafine particles (DLPI unit in the present work vs. SFU unit in Arsene et al. (2011)). Parallel DLPI and SFU sampling runs (performed within January–July 2016) showed that the DLPI unit could collect in average with $\sim 6.7 \mu\text{g m}^{-3}$ more particles than the SFU system. However, in a study from 2016, Alastuey et al. (2016) report for PM₁₀ concentrations in Moldova (the closest point to our sampling site), values as high as $\sim 25 \mu\text{g m}^{-3}$ over summer and of $\sim 25\text{--}30 \mu\text{g m}^{-3}$ over winter period, yielding an annual averaged value of $\sim 27.5 \mu\text{g m}^{-3}$ which is much higher than the $18.9 \mu\text{g m}^{-3}$ value reported in the present work, for Iasi, north-eastern Romania. However, the elevated concentrations observed at the eastern sites were



attributed to regional or local sources (Alastuey et al., 2016). The difference observed in comparison with other European sites might actually reflect that altitude would be an important controlling factor to the atmospheric aerosol burden at a site.

In Iasi, north-eastern Romania, mass concentrations in the 5 to 10 $\mu\text{g m}^{-3}$ range, for the PM_{10} and $\text{PM}_{2.5}$ fractions were especially observed in samples collected after raining events (i.e., May, June, August, and October). Such behaviour would

5 be expected since particles from the atmosphere might be efficiently removed by precipitation (Arsene et al., 2011).

However, during events with strong natural or anthropogenic contributions the PM_{10} and $\text{PM}_{2.5}$ mass concentrations exceeded the averages observed at AMOS. For example, an event collected in April 2016, from 9th to 11th, with 34.3 $\mu\text{g m}^{-3}$ in $\text{PM}_{2.5}$ and 43.9 $\mu\text{g m}^{-3}$ in PM_{10} , was actually highly influenced by the long range transport phenomena of African dust and marine aerosols from the Black and Aegean/Mediterranean seas (i.e., event described in detail later in the text). For other

10 events, the exceeding fine fraction mass concentrations are believed to be a result of more variable sources (combustion, biogenic, local mineral dust, meteorological factors, etc.).

Figure 2 shows monthly arithmetic mean mass concentrations of the PM_{10} and $\text{PM}_{2.5}$ fractions (accompanied by standard deviations) in Iasi, north-eastern Romania. The distribution of the $\text{PM}_{2.5}/\text{PM}_{10}$ ratio is presented in the same figure. The

relative contribution of the $\text{PM}_{2.5}$ toward the PM_{10} particles indicates low variability amongst the months of the year with ratios ranging from ~ 0.75 to ~ 1.0 . For urban background and/or traffic sites $\text{PM}_{2.5}/\text{PM}_{10}$ ratios in the 0.42 to 0.82 range are given by the WHO (WHO, 2006a). Clear seasonal pattern with maxima during the cold seasons and minima during the warm

seasons are attributable to the $\text{PM}_{2.5}$, PM_{10} and $\text{PM}_{2.5}/\text{PM}_{10}$ profiles. The observed seasonal pattern might be the result of combined effects from emissions seasonal variations, local and long range air masses transport and dispersion, chemical production and loss, and deposition (Wang et al., 2016). The higher $\text{PM}_{2.5}/\text{PM}_{10}$ ratios, occurring especially during cold

20 seasons, are most probably due to contributions from combustion processes. During such periods, i.e. coal/petroleum burning for heating purposes, an enhancement of secondary aerosols generation (sulfate and organic compounds) is expected (Li et al., 2012). The lower $\text{PM}_{2.5}/\text{PM}_{10}$ ratios occurring during warm seasons can be due to the increased frequency of dust and

also due to more intense anthropogenic activities in the neighbourhood of the sampling site (excavation, construction, build renewing and not only) which would result in higher loading of coarse particles in the atmosphere. According to Zhang et al.

25 (2001) it might also be that during the warm seasons the growth of plants may enhance the dry deposition of $\text{PM}_{2.5}$ and hence the $\text{PM}_{2.5}/\text{PM}_{10}$ ratio.

However, over the investigated period clear seasonal pattern was observed for the gravimetrically determined mass concentration size distribution (Fig. 3). The average size distribution over the cold seasons presents a clear monomodal feature with maximum at 381 nm. The warm seasons are characterized by the presence of a dominant fine mode, with maxima at 381 nm, but also by the occurrence between 1.60–2.39 μm of a supermicrone mode. Most probably, the observed seasonal variations cannot be attributed solely to changes in sources contributions, but also probably to variations of meteorological conditions.



3.2 Ionic balance, seasonality of water soluble ions and stoichiometry of $(\text{NH}_4)_2\text{SO}_4$ and NH_4NO_3

3.2.1 Ionic balance and potential aerosols acidity

Water soluble inorganic anions (i.e., F^- , Cl^- , NO_2^- , NO_3^- , PO_4^{3-} , SO_4^{2-}), organic anions (i.e., HCO_2^- , $\text{C}_2\text{H}_3\text{O}_2^-$, $\text{C}_2\text{O}_4^{2-}$), and inorganic cations (i.e., Na^+ , K^+ , NH_4^+ , Mg^{2+} , Ca^{2+}) were analyzed by ion chromatography. The completeness degree of the ionic balance for the identified and quantified species in both the PM_{10} and $\text{PM}_{2.5}$ fractions was checked. For raw ion chromatography data slopes lower than unity in the \sum_{cations} vs. \sum_{anions} dependences were observed in both the $\text{PM}_{2.5}$ (total period, averaged ratio of 0.69, Pearson coefficient of 0.94, $p < 0.001$, at the 99.9 % confidence level; cold seasons, ratio of 0.67, Pearson coefficient of 0.98, $p < 0.001$, at the 99.9 % confidence level; warm seasons, ratio of 0.84, Pearson coefficient of 0.87, $p < 0.001$, at the 99.9 % confidence level) and PM_{10} (total period, averaged ratio of 0.70, Pearson coefficient of 0.94, $p < 0.001$, at the 99.9 % confidence level; cold seasons, ratio of 0.68, Pearson coefficient of 0.98, $p < 0.001$, at the 99.9 % confidence level; warm seasons, ratio of 0.86, Pearson coefficient of 0.86, $p < 0.001$, at the 99.9 % confidence level) and these indicate important cation deficit in the ionic balance. It seems that over cold seasons the cation deficit is higher than that over warm seasons and it should be also noted that at the investigated site the RH values went even to ~ 82 % during cold seasons. However, per sampled events either cation or anion deficit has been observed in various stages.

Since ion balance method, thermodynamic equilibrium models, molar ratio, and phase partitioning of certain semi-volatile compounds (e.g., $\text{NH}_3/\text{NH}_4^+$, $\text{HNO}_3/\text{NO}_3^-$, HCl/Cl^-), are methods commonly employed for proton loading in atmospheric particles estimation, the generated data-base was under scrutiny in these regards. Predicting pH is suggested as the best method to analyze also particle acidity (Guo et al., 2015). Usually, the ion balance method is based upon the principle of electroneutrality. Any deficit in measured cationic charge compared to measured anionic charge is usually assumed to be due to the presence of unmeasured protons (H^+) while the reverse is available for unmeasured hydroxyl (OH^-) (Hennigan et al., 2015) or bicarbonate/carbonate ($\text{HCO}_3^-/\text{CO}_3^{2-}$) (Fountoukis and Nenes, 2007).

In the present work, however, $\text{HCO}_3^-/\text{CO}_3^{2-}$ was assigned as the missing anion while NH_4^+ as the major missing cation. The missing $\text{HCO}_3^-/\text{CO}_3^{2-}$ has been estimated as suggested by Arsene et al. (2007) while the rationale previously proposed by Arsene et al. (2011) has been used to estimate the missing NH_4^+ . Within the $\text{NH}_4^+(\text{total})$ fraction (defined as the sum between that derived from raw IC data and the part estimated by using the rationale of Arsene et al. (2011)), the correction for the missing NH_4^+ accounted for about 21.65 ± 25.70 % for the warm seasons while for the cold seasons the correction accounted for about 46.05 ± 18.43 %. However, when estimated missing NH_4^+ has been taken into account a significant improvement in the overall ionic balance (\sum_{cations} vs. \sum_{anions}) was observed for both the $\text{PM}_{2.5}$ (total period, ratio of 0.95, Pearson coefficient of 0.98, $p < 0.001$, at the 99.9 % confidence level; cold seasons, ratio of 0.97, Pearson coefficient of 0.99, $p < 0.001$, at the 99.9 % confidence level; warm seasons, ratio of ~ 0.87 , Pearson coefficient of 0.96, $p < 0.001$, at the 99.9 % confidence level) and the PM_{10} (total period, ratio of 0.95, Pearson coefficient of 0.98, $p < 0.001$, at the 99.9 % confidence level; cold seasons, ratio of 0.98, Pearson coefficient of 0.99, $p < 0.001$, at the 99.9 % confidence level; warm seasons, ratio of 0.86, Pearson coefficient of 0.96, $p < 0.001$, at the 99.9 % confidence level) fractions.



Since in the literature there are suggestions that in the ion balance any deficit in inorganic cations relative to anions is mainly due to the presence of H^+ (Hennigan et al., 2015), in an attempt to investigate whether or not the H^+ species would bring an important contribution within the ionic balance, ISORROPIA-II thermodynamic equilibrium model proposed by Fountoukis and Nenes (2007) has been used in the present work. The model helps deriving (even under constraints) either information related to potential H^+ concentration in the aerosol particles (implicitly also on aerosols pH) or to the liquid water content (if a liquid phase exists), and computed concentrations of gas-phase semi-volatile compounds in equilibrium with the aerosol (e.g., NH_3 , HNO_3 , and HCl) (Hennigan et al., 2015). For the present data-base, ISORROPIA-II model was run in “forward mode” for metastable aerosol. Runs were performed both for NH_4^+ derived from raw IC data and also for the situation when missing ionic species have been indirectly estimated and taken into account ($NH_4^+(\text{total})$ and HCO_3^-/CO_3^{2-} estimated as previously presented). Although use of ISORROPIA-II model runs in forward mode with only aerosol-phase input is highly susceptible for debate, Guo et al. (2015) report also about use of the model under these specific conditions. It seems that under these circumstances the model is less sensitive to measurement error than the reverse mode. However, in Guo’s et al. (2015) work, pHs reported for SCAPE were corrected for the identified bias and the values were increased by 1 to simplify the correction.

Although there is suggestion that in thermodynamic model calculation (a region where the thermodynamic predictions, and assumption of equilibrium, become more accurate) only data with RH exceeding 60 % might be considered (Moya et al., 2002), in the present work ISORROPIA-II was applied over the entire set of data-base regardless RH values (in 2016, at the investigated site, July, August and September were the months with $RH < 40\%$). However, the model was also run at additional 5 to 10 % RH (to that experimentally recorded) in order to check RH potential influence on the envisaged estimations. It has been observed that a change in the RH value with 5 or 10 % would result actually in a pH change with about 2 and, respectively, 3 %. Since in the present work, organic species have been taken into account in the ionic balance it is believed that the bias in the estimated species (especially NH_4^+ and HCO_3^-/CO_3^{2-}) is minimized and implicitly that in inferred H^+ by ISORROPIA-II thermodynamic model.

For Iasi, north-eastern Romania, when ISORROPIA-II estimated H^+ has been taken into account the improvement in the overall ionic balance (in comparison with that derived by considering the $NH_4^+(\text{total})$ fraction) was almost insignificant with an $\sim 2\%$ increase on the \sum_{cations} vs. \sum_{anions} ratio, observed in both the $PM_{2.5}$ and PM_{10} fractions. However, over the warm seasons it seems that neither $NH_4^+(\text{total})$ fraction option nor the one taking into account ISORROPIA-II estimated H^+ concentrations do not lead to a close to 1 ionic balance, with ratios varying between 0.84 and 0.88 for the $PM_{2.5}$ fraction and 0.84 to 0.87 for the PM_{10} fraction. Such observation would not suggest high uncertainty in the accuracy of the ionic species measured values but most probably that some volatile cation species (e.g., amines) were not measured.

However, the relationship between ISORROPIA-II predicted aerosol pH and the ionic balance has been investigated for the present data-base and the results are presented in Fig. 4a. Details in this figure (following features of a traditional titration curve) clearly show that many of the analyzed particles were neutral (dashed lines at 0). A very important fraction of the investigated samples were in the acidic range (particles pH below 3 if aerosol samples were in cation deficit mode) while the



remaining fraction was in the alkaline range (particles pH slightly above 7 if aerosol samples were in anion deficit mode). However, at neutrality it is observed that, indeed as suggested by Hennigan et al. (2015), small uncertainties in the ionic balance (coming mainly from the uncertainty in the measurements) may lead to shifts in pH that span over about 10 pH units. Moreover, the sensitivity in predicted aerosol pH under forward-mode calculation to changes in the aerosol NH_4^+ concentration has been checked and, as shown in Fig. 4b, it seems that the predicted pH might decrease by 2 % when the ionic balance takes into account $\text{NH}_4^+(\text{total})$ concentration. Actually, for about 19 % of the data the aerosol pH differed by less than 1.0 pH unit when $\text{NH}_4^+(\text{total})$ concentrations increased in comparison with NH_4^+ derived from raw IC data (a (35.65 ± 24.92) % increase in NH_4^+ concentration for the entire data-base, a (21.65 ± 25.7) % increase for the warm seasons and a (46.05 ± 18.43) % (mean \pm stdev) increase for the cold seasons). Such change in NH_4^+ concentrations is not unexpected since this is assigned as a highly volatile compound, with high susceptibility to be lost by evaporation. As it will be shown later in the text, meteorological parameters (i.e., RH) could play an important role within NH_4^+ distribution in both during the warm and the cold seasons. In other studies, higher evaporation rates are reported for summer when compared to winter, but during winter low RH values were prevailing (Ianniello et al., 2011; Zhao et al., 2016). Ianniello et al. (2011) report for example that in Beijing, China, about 35 % of fine particulate NH_4^+ was susceptible to evaporate from the sampling filters during winter while about 53 % of fine particulate NH_4^+ was susceptible to evaporate during summer. For the same location, Zhao et al. (2016) report NH_4^+ loss of 6 % and higher losses of NO_3^- and Cl^- .

In Iasi, north-eastern Romania, an important fraction of the total analyzed samples was alkaline while the remaining part was acidic. A more detailed view of the samples pH distribution can be easily cached from the data presented in Fig. 4c-d. It seems that over the warm seasons about 55–56 % of the analyzed samples were alkaline ($\text{pH} > 7$) and about 44–45 % were acidic ($\text{pH} < 7$), with the last fraction mainly distributed in the very strong acidity fraction (~ 35 % of the samples with pH in the 0–3 range and about 2 % with aerosol pH less than 0). Over the cold seasons only 47 % of the total analyzed samples were alkaline ($\text{pH} > 7$) and 53 % were acidic ($\text{pH} < 7$). The acidity was also mainly distributed in the very strong acidity fraction (~ 43 % of the acidic samples with pH in the 0–3 range). However, while during the warm seasons ~ 24 –25 % of the acidic samples has had the pH in the 1–2 range (reflecting actually contributions from very strong inorganic acids), over the cold seasons an increase to ~ 40 %, brought by the 1–3 pH range, would reflect possible contributions from other acidic type species (i.e., organics). Aerosols acidity might actually impact the gas–particle partitioning of semi-volatile organic acids. While under strong acidic conditions (pH in the 1–3 range) organic acids contributions to the H^+ (hence pH) are expected to be negligible (since low pH prevents dissociation of organic acids), at pHs above 3, and well approaching 7, it is believed that their contribution would significantly enhance (see also discussion later in the text). Under these circumstances, in Iasi, north-eastern Romania, the contribution from formic acid, one of the strongest organic acid which has a pK_a of 3.75 (Bacarella et al., 1955) ($\text{pK}_a = -\log K_a$, with K_a referring to acid dissociation constant) might become important over the cold seasons.

Figures 5a,b present the size distribution of averaged aerosol mass, NO_3^- , SO_4^{2-} and NH_4^+ concentrations while Fig. 5c,d present ISORROPIA-II estimated pH and H^+ mass concentration distributions for both the cold (Fig. 5.a,c) and the warm



(Fig. 5b,d) seasons. Clear monomodal distribution seems to be specific for the cold seasons while for the warm seasons the second mode mass concentration distribution seems to be predominated by NO_3^- . For the 155–612 nm size range, from details presented in Fig. 5c,d, it is quite clear that the pH values were at 2 or below 2 pH units. Moreover, in the present work it has been observed that the aerosol H^+ levels, inferred indirectly from the ion balance concept proposed by Hennigan et al. (2015), showed statistically significant correlation with the H^+ loadings predicted by ISORROPIA-II in the forward mode (Pearson coefficient of 0.72, $p < 0.001$, at the 99.9 % confidence level). However, there are discrepancies between the two estimated H^+ levels, with those from thermodynamic model in orders of magnitude lower than those from the ionic balance (most probably due to the fact that the models account only for partial dissociation). It is also believed that estimation of the aerosol H^+ loading from the ionic balance was affected by the uncertainty coming from the propagation of measurement error, especially under conditions where a slight anion deficit balance was inferred as an H^+ loaded system. Under these circumstances this trace could also represent an uncertainty source in H^+ levels estimated from the ion balance. However, overall in our study, conditions of increasing H^+ loadings were corresponding to decreasing aerosol pH and this observation would actually imply that most probably in the 155–612 nm particles size range, the aerosol particles were characterized by strong acidity (i.e., H^+ contributed mainly by completely dissociated strong acids, mainly in the H_2SO_4 and HNO_3 form). Contributions from free acidity (dissociated H^+) or total acidity (free H^+ and undissociated H^+ bound to weak acids) is expected to be more important in all other remaining fraction, and especially in the 27.6–94.5 nm particles size range (see discussion also later in the text). However, it is strongly believed that highly confident estimated aerosol particles pH would allow better prediction in the chemical behaviour of organics especially if taken into account the fact that, at relatively low acidities, organic acids will dissociate, greatly contributing to the ion balance.

In the literature there is suggestion that the molar ratio approach is also often used as a proxy for aerosol pH estimation (Hennigan et al., 2015). However, the procedure is also highly susceptible to bias the results either due to exclusion of minor ionic species or due to the fact that it does not take account for the effects of aerosol water or species activities on particle acidity. In the present work, even under the limiting case when the aerosol regime was inferred to be highly acidic (i.e., samples with $\text{NH}_4^+ / (\text{Cl}^- + \text{NO}_3^- + 2 \times \text{SO}_4^{2-})$ molar ratio less than 0.75), no statistically significant correlation has been observed neither between the cation/anion molar ratio and $[\text{H}^+]$ from the ion balance nor between the molar ratio and forward-mode predictions of aerosol pH. In such conditions it was assumed that the molar ratio would not be a suitable tool to infer the acidity of atmospheric particles at the interest site but it could be a good parameter reliable to distinguish between alkaline and acidic particles.

Although measurements on gaseous NH_3 were not available the potential relationship between $\text{NH}_3/\text{NH}_4^+$ phase partitioning approach (with ISORROPIA-II gaseous NH_3 predicted values) and predicted aerosol particles pH has also been investigated. For further interpretation, equilibrium gas-aerosol system was assumed to exist due to the fact that the length of sampling time-interval (36 h) was significantly exceeding the equilibration time for submicron particles, which is on the order of seconds to minutes (Meng et al., 1995). As previously mentioned, in the present work it has been determined that only limited number of samples possess pH values < 0 while a significant fraction possess pH greatly higher than 0. Moreover,



the ISORROPIA-II thermodynamic model predicted that in the 94.5 and 612 nm size range not all of the NH_3 partitioned in the aerosol phase and also that a significant fraction was present in the gas phase.

For Iasi, north-eastern Romania, using data from ISORROPIA-II runs, predicted NH_3 concentrations suggested values as high as 0.52 ± 0.28 (0.46) $\mu\text{g m}^{-3}$ at $\text{RH} < 40\%$, 0.61 ± 0.26 (0.49) $\mu\text{g m}^{-3}$ at RH in the 40–60 % range and 0.96 ± 0.54 (0.92) $\mu\text{g m}^{-3}$ at $\text{RH} > 60\%$ (mean \pm stdev (median)). These values specific for the warm seasons are smaller than those reported in a modelling study by Backes et al. (2016), which by the reference case and the political NEC 2020-national emission ceilings coming into force 2020/30 scenario predict NH_3 abundances as high as 1.6 to 2.4 $\mu\text{g m}^{-3}$ (data extracted from NH_3 concentration for the reference case, i.e., fig. 3 in Backes et al., 2016, for north-eastern Romania). The 0.96 ± 0.54 (0.92) $\mu\text{g m}^{-3}$ value at $\text{RH} > 60\%$, predominating mainly during cold seasons, seems to be in reasonable agreement with the ≤ 0.8 $\mu\text{g m}^{-3}$ value modelled by Backes et al. (2016) over winter-time period. Moreover, from ISORROPIA-II runs performed at $\text{RH} < 40\%$, it was estimated that $(77.6 \pm 28.4)\%$ or $(79.3 \pm 26.2)\%$ (mean \pm stdev) of the ISORROPIA-II predicted NH_3 value (both for NH_4^+ derived from raw IC data and, respectively, for the NH_4^+ (total) fraction) could be present in the gaseous form. Nitric acid (HNO_3) and hydrochloric acid (HCl) distributions were in average of $(14.9 \pm 23.1)\%$ (when NH_4^+ derived from raw IC data) or $(13.9 \pm 21.4)\%$ (for NH_4^+ (total) fraction) and, respectively, $(7.4 \pm 12.8)\%$ (when NH_4^+ derived from raw IC data) or $(6.8 \pm 11.4)\%$ (for NH_4^+ (total) fraction). In each run an opposite trend was observed between the distribution of the $\text{NH}_3/\text{NH}_4^+$ partition and those specific for the $\text{HNO}_3/\text{NO}_3^-$ and HCl/Cl^- systems.

By increasing the RH , the $\text{NH}_3/\text{NH}_4^+$ partition enhanced, and at RH in the 40–60 % range it could be observed that $(76.5 \pm 30.9)\%$ or $(78.6 \pm 28.2)\%$ (mean \pm stdev) of the ISORROPIA-II predicted NH_3 value (both for NH_4^+ derived from raw IC data and, respectively, for the NH_4^+ (total) fraction) could be present in the gaseous form. The nitric acid distribution in the gas phase could account for $(17.5 \pm 26.9)\%$ or $(16.1 \pm 24.5)\%$ while that for hydrochloric acid was accounted by $(6.0 \pm 11.7)\%$ or $(5.3 \pm 10.0)\%$ for both NH_4^+ concentrations derived from raw IC data and, respectively, for the NH_4^+ (total) fraction.

At $\text{RH} > 60\%$ only $(68.3 \pm 36.7)\%$ or $(74.5 \pm 29.7)\%$ (mean \pm stdev) of the ISORROPIA-II predicted NH_3 value (both for NH_4^+ derived from raw IC data and, respectively, for the NH_4^+ (total) fraction) was susceptible to be present in the gaseous form. The nitric acid distribution in the gas phase could account for $(25.6 \pm 32.5)\%$ or $(20.3 \pm 25.8)\%$ while that for hydrochloric acid was accounted by $(6.1 \pm 10.6)\%$ or $(5.2 \pm 9.0)\%$ for NH_4^+ concentrations derived both from raw IC data and, respectively, for the NH_4^+ (total) fraction. In other studies, thermodynamic equilibrium calculations predicted that all of the NH_3 was mainly susceptible for partitioning to the particle phase at the equilibrium and also that > 44 or 51% of the investigated samples presented aerosols pH less than 0 (Hennigan et al., 2015). It is however believed that at the investigated Romanian site (i.e., Iasi, north-eastern Romania), the atmosphere was enough rich in NH_3 such as to promote its partition into the particle phase and to exist also into gaseous form.

Using data from the ISORROPIA-II thermodynamic model, it has been observed that in the 155 and 612 nm size range (regardless the RH values) the aerosol ammonium fraction ($\text{NH}_4^+ / (\text{NH}_3 + \text{NH}_4^+)$), calculated both for NH_4^+ derived from raw IC data or for the NH_4^+ (total) fraction, was exceeding 0.20 value. Clear maxima of the ($\text{NH}_4^+ / (\text{NH}_3 + \text{NH}_4^+)$) ratio were



observed at 381 nm (0.71 at $RH < 40\%$, 0.63 at RH in the 40–60 % range and 0.76 at $RH > 60\%$ with NH_4^+ derived from raw IC data or 0.66 at $RH < 40\%$, 0.56 at RH in the 40–60 % range and 0.65 at $RH > 60\%$ with NH_4^+ (total) fraction. As seen in Fig. 5c,d, in the 155–612 nm size range, aerosols pH size distribution presents a clear cessation while in the 27.6–94.5 and 612–9940 nm size ranges, aerosol particles pH is often slightly below 8. Although not presented, in the same size range (i.e., 155–612 nm) the aerosol ammonium fraction ($NH_4^+/(NH_3 + NH_4^+)$) shows a significant increase with values as high as almost 1, while in other two size ranges the aerosol ammonium fraction ($NH_4^+/(NH_3 + NH_4^+)$) was very low or close to 0 suggesting to some extent also the existence of gaseous NH_3 . However, such behaviour would actually suggest that at the estimated pH values, enough NH_3 was always present in the gaseous phase such as an important fraction to partition also in the particle phase.

10 3.2.2 Seasonality of major water soluble ions

Table 3 shows at the investigated site (i.e., Iasi, north-eastern Romania) summary statistics (monthly based) for the meteorological variables, PM_{10} and $PM_{2.5}$ mass concentrations and for major water soluble ions mass concentrations in the $PM_{2.5}$ fraction. In the PM_{10} fraction, in comparison with the $PM_{2.5}$ fraction, increases within 13–80 % (35 %) (min–max (mean) in the mass concentration of Cl^- , 1–107 % (32 %) for NO_3^- , 1–170 % (17 %) for SO_4^{2-} , 38–185 % (63 %) for HCO_3^- , 14–171 % (41 %) for acetate, 4–136 % (22 %) or formate, 0–294 % (27 %) for oxalate, 16–48 % (32 %) for Na^+ , 6–58 % (20 %) for K^+ , 1–105 % (12 %) for NH_4^+ (total), 28–83 % (46 %), for Mg^{2+} and 33–123 % (61 %) for Ca^{2+} were observed. However, the PM_{10} and $PM_{2.5}$ mass concentrations fractions show statistically significant correlation with a ratio of 1.1 (Pearson coefficient of 0.99, $p < 0.001$, at the 99.9 % confidence level). Higher mass concentrations of specific water soluble ions (i.e., Cl^- , NO_3^- , K^+ , NH_4^+ and to some extent also SO_4^{2-}) during the cold seasons than during the warm seasons are most probable the result either of the combination of increased strength of pollution sources and meteorological effects (inducing most probable lower mixing heights or even temperature inversion) or of different chemical/photochemical processing. In a study at Kanpur, India, the authors report also higher abundances of particulate NO_3^- , SO_4^{2-} , NH_4^+ , K^+ in winter than in summer but the authors claim that $CaCO_3$ could be mainly responsible on NO_3^- abundance (Sharma et al., 2007).

Seasonal variations for selected water-soluble ionic components in the $PM_{2.5}$ fraction are shown in Fig. 6a–h while Fig. 6i presents the variation of the mixed layer depth at the investigated site. Fine particulate Cl^- , NO_3^- , K^+ , NH_4^+ (total), and to some extent even SO_4^{2-} , seem to exhibit distinct seasonal variations with maxima during the cold seasons and minima over the warm seasons. However, it might be that changes in the mixed layer depth contributed also to the observed seasonality. The summer minima observed for both NO_3^- and NH_4^+ ions is not extremely surprising since their most predominant form, i.e. NH_4NO_3 , is volatile and tends to dissociate and stay in gas phase at high temperatures. Coarse particulate $C_2O_4^{2-}$, Ca^{2+} and Na^+ did not show much variation with respect to seasons. However, SO_4^{2-} and $C_2O_4^{2-}$ show similar pattern (implying most probably common sources) and Ca^{2+} variation reflects possible prevalent contribution from soil dust. Higher winter than summer ion concentrations are reported by Sharma et al. (2007) for Kanpur (India) while Ianniello et al. (2011) report opposite trends for Beijing (China).



Particulate Cl^- mass concentrations show clear seasonal pattern with higher values during the cold seasons than during the warm seasons (Fig. 6a). In both $\text{PM}_{2.5}$ and PM_{10} fractions Cl^- mass concentration correlated statistically significant with RH (Pearson coefficient higher than 0.71, $p = 0.010$, at the 95.4 % confidence level, positive slope), temperature (only for PM_{10} fraction, Pearson coefficient higher than 0.59, $p = 0.045$, at the 95.4 % confidence level, negative slope), particle loading (Pearson coefficient higher than 0.60, $p = 0.038$, at the 95.4 % confidence level, positive slope) and mixed layer depth (Pearson coefficient higher than 0.69, $p = 0.012$, at the 95.4 % confidence level, negative slope). Its maxima during the cold seasons might be the result of increased coal burning activities for heating purposes or due to the use of NaCl in winter to avoid the effects of slippery roads. These observations are in agreement with those of other studies conducted at eastern European sites (Arsene et al., 2011; Alastuey et al., 2016). However, Cl^- mass concentration follows similar pattern with that of K^+ (tracer of biomass burning) allowing us suggesting that over the cold seasons wood burning might become an important heating source (Christian et al., 2010; Akagi et al., 2011).

As seen in both Table 3 and Fig. 6b, NO_3^- ion presents clear temporal pattern with maxima during the cold seasons and minima during the warm seasons. The inset distribution presented within NO_3^- seasonal variation (Fig. 6b) is clearly reflecting that over the warm seasons the coarse fraction, in comparison with fine fraction, might also bring significant contributions to the aerosol atmospheric burden. In our work fine particulate NO_3^- mass concentrations varied from 0.31 to 3.62 $\mu\text{g m}^{-3}$ (Table 3) and these data are in very good agreement with those predicted for Europe in a modelling study performed by Backes et al. (2016). The data measured in the present work over the cold seasons ($3.62 \pm 1.10 \mu\text{g m}^{-3}$ over January, February, December as the coldest months of the year and $2.65 \pm 0.38 \mu\text{g m}^{-3}$ over January, February, March, October, November, December; averaged data from Table 3) seem to be in reasonable good agreement with those predicted for Europe in the modelling study performed by Backes et al. (2016) (abundances predicted by the reference case and the political scenario NEC 2020-national emission ceilings coming into force 2020/30 in the 2.4 to 3.2 or even higher $\mu\text{g m}^{-3}$ range over winter; data extracted from NO_3^- concentration in $\text{PM}_{2.5}$, i.e., fig. 5 in Backes et al., 2016, for north-eastern Romania). The $0.59 \pm 0.30 \mu\text{g m}^{-3}$ NO_3^- measured concentration in $\text{PM}_{2.5}$ over warm seasons (including April month characterized by predominant air masses buoyancies events; $0.44 \pm 0.12 \mu\text{g m}^{-3}$ NO_3^- measured concentration without April month) is lower than that predicted by Backes et al., (2016) model (abundances as high as 0.8 $\mu\text{g m}^{-3}$ over the summer) and, as in NH_4^+ case, this might reflect the susceptibility of NO_3^- to be mainly transferred in the gas phase over the warm seasons. From the data presented in Table 3 it has been also observed that NO_3^- mass concentrations, in both $\text{PM}_{2.5}$ and PM_{10} fractions, correlated statistically significant with RH values (Pearson coefficient higher than 0.84, $p < 0.001$, at the 99.9 % confidence level, positive slope), temperature (Pearson coefficient higher than 0.92, $p < 0.001$, at the 99.9 % confidence level, negative slope), mixing layer depth (Pearson coefficient higher than 0.84, $p < 0.001$, at the 99.9 % confidence level, negative slope) and particles loading (Pearson coefficient higher than 0.65, $p = 0.021$, at the 95.4 % confidence level, positive slope) in both $\text{PM}_{2.5}$ and, respectively, PM_{10} fractions. However, as previously presented, since highly acidic aerosols are expected over all seasons this will most probably affect a variety of processes and definitely the partitioning of HNO_3 to the gas phase, resulting in low nitrate aerosol levels. Guo et al. (2015) report also low nitrate aerosol levels during



summer. Moreover, since NO_3^- heterogeneous formation (i.e., condensation or absorption of NO_2 in moist aerosols or N_2O_5 oxidation and HNO_3 condensation) generally relates to RH and the particulate loading (Wang et al., 2006; Ianniello et al., 2011) it is believed that at the investigated site this process might be of similar importance as gas–particle conversion (implying mainly oxidation by photochemical processes of precursor gases, such as NO_x , to nitrate via HNO_3 formation).

5 The high concentration of NO_3^- during the cold seasons might also be due to higher concentrations of NH_3 in the atmosphere, from unaccounted yet sources, available to neutralize H_2SO_4 and HNO_3 (as will be later shown in the text). Moreover, the high relative humidity conditions over the cold seasons could offer suitable conditions such as significant fractions of HNO_3 and NH_3 to be dissolved in humid particles, therefore enhancing fine particulate NO_3^- and NH_4^+ in the atmosphere (Pathak et al., 2009, 2011; Ianniello et al., 2010; Sun et al., 2010). Kai et al. (2007), from measurements
10 performed in October 2004 in Beijing, China, concluded also that higher RH, higher stable atmosphere structure and higher concentration of NH_3 can lead to a higher transformation ratio of NO_x to NO_3^- .

For particulate SO_4^{2-} maxima are observable during the cold seasons but also during the warm seasons. However, SO_4^{2-} mass concentrations didn't show statistically significant correlation with any of the measured meteorological parameters. From the data presented in Fig. 6c it can be observed that its monthly mean mass concentrations seasonality seems to be not
15 that clear as that of NO_3^- and NH_4^+ suggesting also a possible regional characteristic of SO_4^{2-} formation (Wang et al., 2016). In Iasi, north-eastern Romania, higher SO_4^{2-} concentrations during the cold seasons may be due to increased coal and wood burning combined with poor dispersion (low mixed layer depth) and high RH values. High relative humidity is seen as important factor responsible for the conversion of SO_2 to SO_4^{2-} (Kadowaki, 1986) with a significant enhancement of SO_4^{2-} production rate in aqueous phase (Sharma et al., 2007). Over the warm seasons the temporal trend observed for SO_4^{2-} is
20 thought to be induced by the high rate of photochemical activity (although not shown, higher solar radiation intensity and temperature measured at AMOS) and atmospheric oxidation (most probably high oxidant concentration, such as OH radicals) which increases the oxidation of SO_2 and its conversion rate to SO_4^{2-} (Stelson and Seinfeld, 1982; Stockwell and Calvert, 1983; Kadowaki, 1986; Wang et al., 2005).

As for particulate $\text{NH}_4^+(\text{total})$, both the data in Table 3 and Fig. 6f show that this chemical species presents clear seasonal
25 pattern with maxima during the cold seasons and minima over the warm seasons, observation in agreement with reports at other European (Schwarz et al., 2012; Bressi et al., 2013; Tositti et al., 2014; Voutsas et al., 2014) or non-European sites (Sharma et al., 2007; Wang et al., 2016). The behaviour seems to be opposite to Ianniello et al. (2011) report and this might be due to the fact that changes in the mixed layer depth (as seen in Fig. 6i) played a very important role in its distribution. Although NH_4^+ is expected to present enhanced evaporation over warm seasons, it seems that in Iasi, north-eastern Romania,
30 an important fraction of the particulate NH_4^+ (~ 45 %) is lost during the cold seasons mainly due to the influence of meteorological parameters such as those inducing emissions from dew evaporation with fast temperature increase (see also discussion later in the text). Higher particulate NH_4^+ abundances over the cold seasons (although a maximum is expected over the warm seasons) are mainly related to changes in the mixed layer depth all around the year (i.e., mixed layer depth



development associated with dilution effect responsible for the warm seasons minima, while lower mixed layer depth associated with accumulation effect responsible for the cold seasons maxima).

In our work $\text{NH}_4^+(\text{total})$ measured concentration varied from 0.8 to 2.09 $\mu\text{g m}^{-3}$, a range which is much lower than that reported by Meng et al. (2011) for a more polluted site (i.e., Beijing, China, with concentrations varying between 4.73 to 9.04 $\mu\text{g m}^{-3}$ within various seasons). However, the data measured in the present work over the cold seasons ($2.03 \pm 0.30 \mu\text{g m}^{-3}$ over January, February, December as the coldest months of the year and $1.65 \pm 0.23 \mu\text{g m}^{-3}$ over January, February, March, October, November, December; averaged data from Table 3) seem to be in reasonable good agreement with those predicted for Europe in a modelling study performed by Backes et al. (2016) (abundances predicted by various models in the 1.6 to 2.4 $\mu\text{g m}^{-3}$ range over winter; data extracted from NH_3 concentration for the reference case, i.e., fig. 4 in Backes et al., 2016, for north-eastern Romania). The $0.90 \pm 0.09 \mu\text{g m}^{-3}$ $\text{NH}_4^+(\text{total})$ measured concentration over warm seasons is much lower than that predicted by Backes et al., (2016) model (abundances as high as 1.6 $\mu\text{g m}^{-3}$ over the summer) but the discrepancy might actually reflect the limitation of the experimental measurement techniques in regard to NH_4^+ volatility.

Moreover, in Iasi, north-eastern Romania, it has been also observed that $\text{NH}_4^+(\text{total})$ mass concentration correlated statistically significant with RH values (Pearson coefficient higher than 0.80, $p = 0.001$, at the 95.4 % confidence level, positive slope), temperature (Pearson coefficient higher than 0.85, $p < 0.001$, at the 99.9 % confidence level, negative slope, temperature increase causing particulate $\text{NH}_4^+(\text{total})$ mass concentration decrease), mixed layer depth (Pearson coefficient higher than 0.80, $p = 0.001$, at the 95.4 % confidence level, negative slope, mixed layer depth increase causing particulate $\text{NH}_4^+(\text{total})$ mass concentration decrease), and particle loading (Pearson coefficient higher than 0.64, $p = 0.023$, at the 95.4 % confidence level, positive slope) in both $\text{PM}_{2.5}$ and, respectively, PM_{10} fractions. $\text{PM}_{2.5}$ fraction showed statistically significant correlation also with the mixing depth (Pearson coefficient higher than 0.67, $p = 0.016$, at the 95.4 % confidence level).

The seasonal variation of particulate $\text{NH}_4^+(\text{total})$ follows especially those of particulate NO_3^- and Cl^- , which would indicate that most probably $\text{NH}_4^+(\text{total})$ largely originates from the neutralization between NH_3 and acidic species of the afore mentioned ions (Wang et al., 2006) or that the species were likely internally mixed and came from similar gas-to-particle processes (Huang et al., 2010). Although in the present work gaseous NH_3 was not measured, ISORROPIA-II thermodynamic equilibrium model runs predicted that at the investigated site the atmosphere was often in gaseous ammonia-rich state regardless the RH values (the $[\text{NH}_3]/([\text{HNO}_3] + [\text{HCl}])$ strongly exceeding 1). Studies undertaken over various seasons (but with RH values predominantly below 50 % over the cold and > 70 % over the warm seasons) showed that temperature presented a significant positive correlation with NH_3 , a behaviour suggesting actually that high temperature would facilitate NH_3 release from its sources while both low wind speed and low mixed layer depth would cause intensive atmospheric stability, limiting the dispersion of air pollutants (Zhao et al., 2016). ISORROPIA-II runs predicted for NH_3 in Iasi, north-eastern Romania, values as high as 0.96 ± 0.54 (0.92) $\mu\text{g m}^{-3}$ at $\text{RH} > 60$ % often prevailing over the cold season, which were significantly higher than those estimated for other RH values and higher temperatures. It might be that over cold seasons, at the interest location, the meteorological parameters would play a more important role than expected in the



physico-chemical processes controlling the atmospheric burden of chemical species. Since over the cold seasons RH values were as high as almost 69 % it is supposed that at this high RH value the dew point was closer to the current air temperature. Moreover, over the cold seasons at the investigated site, changes of about 10 °C in the ambient temperature from day-to night were quite often experienced and such a large driving force it is believed actually to enhance the evaporation rate process which would become the limiting step controlling NH_4^+ abundance in both particulate and gaseous phase. In the atmosphere, gaseous NH_3 concentration, concentrations of atmospheric acidic gases, characteristics of pre-existing aerosols, air temperature, and humidity are supposed to play a significant role in generating particulate NH_4^+ . In a study performed by Zhao et al. (2016), the authors report about the fact that NH_3 to NH_4^+ conversion was favoured under the conditions of low temperature and high relative humidity. It might be that also in our study, high NH_3 ISORROPIA-II estimated level (under cold associated very high RH conditions) is the factor of utmost importance facilitating fine particulate ammonium salt formation during this period of the year. However, in overall particulate NH_4^+ (total) associated mainly with NO_3^- and SO_4^{2-} in both $\text{PM}_{2.5}$ and PM_{10} fraction and therefore it is suggested that enhanced fine particulate ammonium salt formation due to available NH_3 could be an important cause of $\text{PM}_{2.5}$ and PM_{10} pollution in the urban atmosphere of Iasi, north-eastern Romania.

It has been observed that at the investigated site $\text{C}_2\text{O}_4^{2-}$ and SO_4^{2-} ions present similar behaviour and $\text{C}_2\text{O}_4^{2-}$ maxima during summer may suggest photochemical and/or biogenic contribution to its abundance (Laongsri and Harrison, 2013). Sodium ion, tracer of sea-salt or NaCl aerosols, shows higher concentrations during spring, a season highly predominated by long range transport of air masses from S-SE sector with contributions from natural sources, especially sea-spray aerosols from the Black Sea. Particulate K^+ mass concentrations show also clear seasonal pattern with higher values during cold than during the warm seasons (Fig. 6e), and this could be due to increased wood burning process corroborated with the height of the mixed layer depth. However, particulate K^+ mass concentrations revealed also some maxima during the months with intense agricultural biomass burning for field clearing (i.e., April, July, and September). It has been observed that K^+ mass concentrations follows similar pattern with that of Cl^- (Pearson coefficient of 0.79, $p = 0.002$, at the 95.4 % confidence level) but not with that of SO_4^{2-} allowing us to suggest that intense wood burning might be a possible common source for K^+ and Cl^- species (Christian et al., 2010; Akagi et al., 2011).

High mass concentrations of Ca^{2+} and Mg^{2+} (with Mg^{2+} shown only in Table 3 but not in Fig. 6), as soil/dust tracers, were observed especially in spring and summer. Over these seasons, cessation in precipitation frequency and high wind speed contribute to the observed behaviour. During cold seasons, low wind speeds might prevent soil getting reborn in the atmosphere and hence lower values for these ions during these periods of the year. However, Mg^{2+} and Ca^{2+} as mineral ions did not show any correlations neither with $\text{PM}_{2.5}$ nor with PM_{10} fractions and these observations allows us suggesting that most probable NH_3 rather than mineral ions would play a more important role in inorganic secondary particle formation.



3.2.3 Stoichiometry of $(\text{NH}_4)_2\text{SO}_4$, NH_4NO_3 and NH_4Cl

Table 4 presents the correlation matrix (Pearson coefficients) for major ionic species (Cl^- , NO_3^- , SO_4^{2-} , CH_3COO^- , HCOO^- , $\text{C}_2\text{O}_4^{2-}$, HCO_3^- , Na^+ , $\text{NH}_4^+(\text{total})$, K^+ , Mg^{2+} , Ca^{2+}) in $\text{PM}_{2.5}$ aerosol particles both for the cold seasons (Table 4.a) and the warm seasons (Table 4.b). Although similar correlations have been observed also for the PM_{10} fraction, for the correlation matrix analysis $\text{PM}_{2.5}$ fraction has been selected as this is the most representative. For the cold seasons, data in Table 4.a shows significant correlations among many chemical pairs (at the 99.9 % confidence level). It might be that at lower temperatures chemical species such as $(\text{NH}_4)_2\text{SO}_4$, NH_4NO_3 , $(\text{NH}_4)_2\text{C}_2\text{O}_4$, and other associations are formed in the atmosphere with significant contributions to $\text{PM}_{2.5}$ fraction. Over the warm seasons $(\text{NH}_4)_2\text{SO}_4$, $\text{Mg}(\text{NO}_3)_2$, and NaCl chemical associations seems to be the most important. However, $\text{Ca}(\text{HCO}_3)_2$ might play a role in both during the cold and warm seasons. Over the cold seasons it has been also observed that K^+ ion showed statistically significant correlation with many inorganic (NO_3^- , Cl^- and SO_4^{2-}) and organic (HCOO^- and $\text{C}_2\text{O}_4^{2-}$) anions. Such observations allow us suggesting that these species might have common biomass burning sources known to consist mostly of internally mixed potassium salts (K_2SO_4 , KNO_3 , KCl and probably HCOOK and $\text{K}_2\text{C}_2\text{O}_4$) (Ianniello et al., 2011 and references therein).

In ambient atmosphere, inorganic ammonium salts such as ammonium bisulfate (NH_4HSO_4), ammonium sulfate ($(\text{NH}_4)_2\text{SO}_4$), ammonium nitrate (NH_4NO_3), and ammonium chloride (NH_4Cl) are known to be produced by gas-to-particle conversion processes. In the present work, from the ionic balance analysis NH_4^+ ion was assigned as the most critical parameter in the chemical composition analysis of aerosol particles in Iasi, north-eastern Romania (with 274 analysed samples representing 25 % from the total, i.e. 1092, highly deficient in cations). However, as previously presented, when the missing NH_4^+ (estimated by undertaking the procedure suggested by Arsene et al., 2011) has been taken into account the ionic balance has significantly improved. Moreover, as a depth inside investigation procedure, NH_4^+ potential neutralization factor, defined as the molar ratio of NH_4^+ to the theoretical one, assuming almost complete conversion of acidic species (H_2SO_4 , HNO_3 and HCl) to $(\text{NH}_4)_2\text{SO}_4$, NH_4NO_3 and NH_4Cl , was under scrutiny in the present work.

Figures 7a,b present the relationship between molar concentrations of fine particulate NH_4^+ (i.e., from raw IC data and also in the total form estimated under the assumptions from Arsene et al., 2011), and that of particulate SO_4^{2-} for both the cold (Fig. 7a) and warm (Fig. 7b) seasons. The correlations between molar concentrations of particulate NH_4^+ and SO_4^{2-} are statistically significant in either situations (cold seasons, NH_4^+ from raw IC data, Pearson coefficient of 0.97, $p < 0.001$, at the 99.9 % confidence level, and for $\text{NH}_4^+(\text{total})$, Pearson coefficient of 0.96, $p < 0.001$, at the 99.9 % confidence level; warm seasons, NH_4^+ from raw IC data, Pearson coefficient of 0.98, $p < 0.001$, at the 99.9 % confidence level and for $\text{NH}_4^+(\text{total})$, Pearson coefficient of 0.97, $p < 0.001$, at the 99.9 % confidence level).

While for raw data, both during the cold and warm seasons, the molar ratios are either slightly higher or lower than 1, for $\text{NH}_4^+(\text{total})$ the ratio is 1.76 for the cold seasons and 1.02 for the warm seasons. These observations would allow us suggesting the existence of enough NH_3 for complete neutralization of H_2SO_4 and also a predominance of particulate $(\text{NH}_4)_2\text{SO}_4$ in agreement with Ianniello et al. (2011) observations. Moreover, as shown in Table 4, for particulate SO_4^{2-} and



NH_4^+ (total) ions pair the correlation was statistically significant (with Pearson coefficients of 0.96, $p < 0.001$ for cold and 0.97, $p < 0.001$ for warm seasons, at 99.9 % confidence level) suggesting that $(\text{NH}_4)_2\text{SO}_4$ could be formed by the reaction of $\text{H}_2\text{SO}_4(\text{g})$ with $\text{NH}_3(\text{g})$ in either situations. However, the 1.76 value for the $[\text{NH}_4^+](\text{total})/(2 \times [\text{SO}_4^{2-}])$ molar ratio during the cold seasons will indicate that there should still be particulate NH_4^+ potentially available to combine with other anions (or
5 existence of enough excess ammonia to neutralize acidic species such as HNO_3 and HCl). Zhao et al. (2016) report $[\text{NH}_4^+]/(2 \times [\text{SO}_4^{2-}])$ molar ratio of 1.54 ($R^2 = 0.63$) with an average ratio of 2.08, indicating the complete neutralization of H_2SO_4 and a predominance of $(\text{NH}_4)_2\text{SO}_4$ in sulfate salts during the cold seasons.

In the present work it has been observed that particulate NO_3^- is the major inorganic species in the 0.155–0.612 μm fraction, especially during months with very high RH. Moreover, the relationship between NO_3^- and SO_4^{2-} , in both the slopes and
10 correlation coefficient terms, was much better over the cold seasons than over the warm seasons. For $(\text{NH}_4^+, \text{SO}_4^{2-})$ ions pair the correlation was statistically significant only during the cold seasons. These observations would allow us suggesting that over these seasons heterogeneous formation of particulate NO_3^- was probably more important than homogeneous formation route.

Unfortunately, at present, no measured NH_3 values are available for the interest site but it is still believed that in the
15 atmosphere of Iasi, north-eastern Romania, sufficient NH_3 in air exists such as significantly to promote both the homogeneous and heterogeneous formation of NO_3^- in the collected aerosol particles. Its formation routes might involve either homogeneous reaction between gaseous HNO_3 and NH_3 (expected to predominate over the warm seasons) (Ianniello et al., 2011) or the heterogeneous reaction between NH_3 and the products formed through the hydrolysis of potential present N_2O_5 on the surface of the pre-existing moist aerosols under relatively high humidity (Pathak et al., 2011; Shon et al., 2013).
20 Actually, in the atmosphere gaseous NH_3 can influence both the aerosol phase inorganic ions but also the aqueous phase hydronium ion (H^+) distribution in aerosols. The concentration of H^+ in aqueous aerosols, or pH, is mainly determined by the balance of acidic ionic components with basic ones. During our measurements period, the atmosphere of Iasi, north-eastern Romania, most probably was frequently abundant with enough NH_3 since, during both the cold and warm seasons, almost half (or slightly higher) of the collected samples were found alkaline with pH values fluctuating between 7 and 8. The
25 remainder samples were acidic and presented pH values ranging mainly from 1 to 3. Zhao et al. (2016) report also about the fact that, on average, a ± 25 % perturbation in NH_3 level could lead to a 0.14 unit pH increase for 25 % perturbation above the measured value and a 0.23 unit pH decrease for a perturbation below the measured value (75 % case). The authors concluded that the relatively flat increasing tendency of pH with increasing NH_3 level reflected and supported their conclusion that sufficient NH_3 was frequently present in wintertime atmosphere and also that the fine collected particulates
30 were almost fully neutralized by NH_3 .

Figures 7c,d,e,f show the relationship between molar concentrations of fine particulate NH_4^+ and sum of the molar concentrations of fine particulate SO_4^{2-} and NO_3^- (Fig. 7c,d) and, respectively, fine particulate NH_4^+ and the sum of the molar concentrations of fine particulate SO_4^{2-} , NO_3^- and Cl^- (Fig. 7e,f) for both the cold and warm seasons. From details given in Fig. 7c,d,e,f it can be easily observed that NH_4^+ , in both derived from raw IC data and total forms, was in deficit



over the cold and warm seasons and under these circumstances it is believed that both particulate NO_3^- and Cl^- could be associated with other alkaline species or be part of acidic aerosol. Since the neutralizing capacity of NH_4^+ toward SO_4^{2-} , NO_3^- and Cl^- acidic species might give a rough indication about potential particles acidity (Li et al., 2015) from Fig. 7c,d,e,f it is quite clear that at AMOS site, if NH_4^+ in derived from raw IC data is used, the neutralization ratios in the investigated particles are less than unity, suggesting that atmospheric particles are most likely acidic and also that a more complex chemistry is ongoing in regard with HNO_3 and HCl species. However, when $\text{NH}_4^+(\text{total})$ (defined as the sum between that derived from raw IC data and the part estimated by using the rationale of Arsene et al. (2011)) the ratios approaches 1 suggesting a possible complete neutralization of particles acidity. From details in Fig. 7e,f it can be easily seen that even for the $[\text{NH}_4^+]$ and $(2 \times [\text{SO}_4^{2-}] + [\text{NO}_3^-] + [\text{Cl}^-])$ molar ratio, actually the available NH_4^+ is not being enough to compensate for other species. However, it should be noted that the Cl^- is not significantly influencing the neutralization of the PM_{10} particles acidity. In a study performed by Zhao et al. (2016) the authors reported $[\text{NH}_4^+]/(2 \times [\text{SO}_4^{2-}] + [\text{NO}_3^-])$ molar ratio of 0.86 ($R^2 = 0.78$) with an average ratio of 1.05, and an $[\text{NH}_4^+]/(2 \times [\text{SO}_4^{2-}] + [\text{NO}_3^-] + [\text{Cl}^-])$ molar ratio of 0.60 ($R^2 = 0.86$) with an average ratio of 0.67). Details presented in Fig. 7c,d clearly show that when $\text{NH}_4^+(\text{total})$ is taken into account a complete neutralization of H_2SO_4 and HNO_3 can be achieved during the cold seasons (Fig. 7c) while during the warm seasons (Fig. 7d) the molar ratio is becoming slightly lower than 1 (i.e., 0.95). During the warm seasons, according to Seinfeld and Pandis (1998), high temperature and low relative humidity would be favourable for NH_4^+ to reach a minimum concentration since it will mainly be transformed into NH_3 and, actually, temperature $> 25^\circ\text{C}$, such as those often encountered at the investigated site over the warm seasons, are known to prevent formation of significant amount of particulate NH_4NO_3 (Adams et al., 1999). Under these circumstances, a cessation in the $[\text{NH}_4^+(\text{total})]/([\text{NO}_3^-] + 2 \times [\text{SO}_4^{2-}])$ molar ratio is to be expected since a significant fraction of the available particulate NH_4^+ will be in equilibrium with gaseous NH_3 . Moreover, at the investigated site, during the cold seasons temperature and relative humidity were of $5.3 \pm 3.9^\circ\text{C}$ and, respectively, $(65.3 \pm 12.8)\%$ and, according with details presented in Table 4, the $(\text{NO}_3^-, \text{NH}_4^+(\text{total}))$ pair presented significant correlation (with Pearson coefficient of 0.98, $p < 0.001$, at the 99.9 % confidence level) only during the cold seasons (low temperature and high relative humidity being favourable for particulate NH_4NO_3 formation, Stelson and Seinfeld, (1982)). During the warm seasons (temperature and relative humidity of $18.9 \pm 3.8^\circ\text{C}$ and, respectively, $40.5 \pm 7.7\%$) the $(\text{NO}_3^-, \text{NH}_4^+(\text{total}))$ pair correlation is of very poor significance most probably due to the influence of meteorological conditions which were not favourable for particulate NH_4NO_3 formation (increasing temperature and decreasing relative humidity limit the production of NH_4NO_3 aerosol (Matsumoto and Tanaka 1996; Utsunomiya and Wakamatsu 1996; Alastuey et al. 2004)).

As presented in Sect. 3.2.2, at the investigated site reductions in NO_3^- and SO_4^{2-} abundances were observed over warm seasons and these may cause increases in gas phase NH_3 with potential more NH_3 deposited closer to emission sites, and therefore decreased sensitivity of inorganic $\text{PM}_{2.5}$ to NH_3 over these seasons. However, as an important aerosol fraction was initially acidic, reductions in SO_4^{2-} is also expected to cause some NH_3 to become available for NH_4NO_3 formation, which could increase the sensitivity of $\text{PM}_{2.5}$ to NH_3 emissions. Actually in the atmosphere, H_2SO_4 and HNO_3 both are known to compete for reacting with NH_3 to form $(\text{NH}_4)_2\text{SO}_4$ and NH_4NO_3 . The reaction rate constant of $(\text{NH}_4)_2\text{SO}_4$ aerosol formation



(by an irreversible reaction due to H_2SO_4 affinity for NH_3), known to be as high as $1.5 \times 10^{-4} \text{ sec}^{-1}$ (Harrison and Kitto, 1992), is almost similar with the reaction rate constants for NH_4NO_3 formation (by a balanced reaction due to NH_3 affinity for HNO_3), which is of the order of $1.59 \times 10^{-4} \text{ m}^3 \mu\text{mol}^{-1} \text{ s}^{-1}$ (Pandolfi et al., 2012; Behera et al., 2013). However, both reaction rate constants are much higher than that between NH_3 and HCl ($5.16 \times 10^{-5} \text{ m}^3 \mu\text{mol}^{-1} \text{ s}^{-1}$) (Behera and Sharma, 2012) and this is what most probably dictates the competition of any of the particulate SO_4^{2-} , NO_3^- and Cl^- for the available NH_4^+ . Usually, when sufficient amount of NH_3 is available (for neutralization of H_2SO_4 and HNO_3), fine mode $(\text{NH}_4)_2\text{SO}_4$ and NH_4NO_3 will be formed via reactions R1 (Cziczo et al., 1997; Zhang et al., 2015) and R2 (Fountoukis and Nenes, 2007; Zhang et al., 2015),



while, when NH_3 limited environment, coarse mode NO_3^- will be formed through reaction R3 involving Mg^{2+} (not Ca^{2+}) mineral ion,



During the warm seasons, however, higher concentrations of $(\text{NH}_4)_2\text{SO}_4$ compared to NH_4NO_3 are expected since $(\text{NH}_4)_2\text{SO}_4$ is less volatile than NH_4NO_3 (Utsunomiya and Wakamatsu, 1996) and, moreover, NH_4NO_3 will form only when available excess NH_3 will react with HNO_3 . Backes et al. (2016), from their modelling study, suggest that a reduction of NH_3 emissions by 50 % may lead to a 24 % reduction of the total $\text{PM}_{2.5}$ concentrations in northwest Europe, with the reduction mainly driven by reduced formation of NH_4NO_3 . However, even in the case of assuming a drastic reduction of NH_3 , the over Europe NH_3 concentration in the atmosphere seems to be high enough to saturate the reaction forming SO_4^{2-} particles, but in contrary to the reaction with H_2SO_4 , the NH_3 concentration in the atmosphere will not be high enough to saturate the reaction with HNO_3 to form NH_4NO_3 particles. The reduced formation of NH_4NO_3 particles may leads to a shift towards gas phase HNO_3 which is intensified in winter. In our study, from ISORROPIA-II thermodynamic model higher shifts towards gas phase HNO_3 have been estimated at higher RH values which were mainly prevailing during cold seasons. The elevated concentration of gas phase HNO_3 may lead to an increased condensation onto existing particles such as sodium chloride (NaCl), and the replacement of Cl^- with NO_3^- may result in an increasing gas phase concentration of HCl in the atmosphere (similar processes described also in Arsene et al. (2011)).

Since in the atmosphere, apart NH_4NO_3 and NH_4Cl salts, other less volatile nitrate and chloride containing species might be also present, the potential of the fine particulate NO_3^- and Cl^- to be chemically bound as relatively non-volatile salts of Ca^{2+} , Mg^{2+} , K^+ or Na^+ , has been also investigated. The free NO_3^- and Cl^- concentrations, defined as the fractions of nitrate and chloride in excess which are not bound with the alkali or alkaline earth metals, have been estimated for both the cold and warm seasons according to the concept described in Ianniello et al. (2011). Zero or negative values of free NO_3^- and Cl^- imply that NH_4NO_3 and NH_4Cl are not present. From the estimated free NO_3^- and Cl^- concentrations, with similar contributions in both the $\text{PM}_{2.5}$ and PM_{10} fractions (i.e., over cold seasons $6.5\text{E}-03 \pm 7.9\text{E}-03 \mu\text{mol m}^{-3}$ ($0.4 \pm 0.5 \mu\text{g m}^{-3}$) for NO_3^- and negative values for free Cl^- ; over the warm seasons $1.6\text{E}-03 \pm 1.8\text{E}-03 \mu\text{mol m}^{-3}$ ($0.1 \pm 0.1 \mu\text{g m}^{-3}$) for NO_3^-



and negative values for free Cl^- , mean \pm stdev), allow us suggesting the potential presence of NH_4NO_3 especially during the cold seasons but not of NH_4Cl neither during the cold nor during the warm seasons. During the cold seasons, particulate NO_3^- didn't show correlation neither with Ca^{2+} nor with Mg^{2+} , but it showed significant correlation with K^+ ($r = 0.85$, $p < 0.001$, at the 99.9 % confidence level from Table 4), indicating possible formation of non-volatile KNO_3 salt along with

5 NH_4NO_3 . Over the warm seasons, fine particulate NO_3^- didn't show correlation with K^+ , but it showed significant correlation with Na^+ and Mg^{2+} ($r = 0.71$, $p < 0.001$ and $r = 0.86$, $p < 0.001$ at the 99.9 % confidence level, from Table 4), indicating possible formation of non-volatile NaNO_3 and $\text{Mg}(\text{NO}_3)_2$ but not of $\text{Ca}(\text{NO}_3)_2$ salts. Since over the warm seasons fine particulate NO_3^- didn't show correlation with NH_4^+ (expected at high temperatures) but it showed statistically significant correlation with HCO_3^- ($r = 0.63$, $p < 0.001$ at the 95.4 % confidence level, from Table 4) these observations would actually

10 suggest possible formation of particulate NO_3^- rather via mineral route than via homogeneous reactions. The significant correlation of fine particulate NO_3^- with Mg^{2+} during the warm seasons ($r = 0.86$, $p < 0.001$ at the 99.9 % confidence level, from Table 4) could increase as importance due to the fact that, as NH_4^+ was not available, neutralization of HNO_3 could occur on coarse soil-driven particle rich in Mg^{2+} (Matsumoto and Tanaka, 1996; Utsunomiya and Wakamatsu, 1996; Alastuey et al., 2004).

15 In the present work moreover, the relative humidity at deliquescence (RHD, which is the relative humidity at which solid particles liquefy) was (65.6 ± 2.0) % over warm seasons, while that over the cold seasons was of (74.1 ± 2.7) %. From the literature it is already known that species such as $(\text{NH}_4)_2\text{SO}_4$ and NH_4HSO_4 , at room temperature, uptakes water (deliquesces) at RH of (79 ± 1) % and, respectively, at RH of 39 % (Cziczo et al., 1997). While until a very low RH (33 ± 2 %, crystallization point) is reached $(\text{NH}_4)_2\text{SO}_4$ aerosol particles might remain in “metastable” or supersaturated state liquid

20 phase (only thereafter a solid might be formed), for NH_4HSO_4 it has been shown that solid phase is difficult to form. In the present work it might be that only over July (RH of 32.95 %), August (RH of 37.12 %) and September (RH of 31.56 %) months formation of solid $(\text{NH}_4)_2\text{SO}_4$ or NH_4HSO_4 could occur.

Pure NH_4NO_3 deliquesces at 62 % RH and there is suggestion that sometime even at 8 % RH the crystallization point is not reached (Dougle et al., 1998). However, according to suggestions from the literature, only during months for which the

25 ambient RH values are less than RHD values the NH_4NO_3 is considered as a solid (Seinfeld and Pandis, 1998). In the present work, from March to October, the ambient RH was always lower than the RHD and therefore, within this period, NH_4NO_3 is assumed to exist to some extent in equilibrium with the solid phase. Within all other months, from the estimated RHD values, there is a small possibility such as NH_4NO_3 to exist also in equilibrium with the aqueous phase and deliquescent particles. However, most probably in Iasi, north-eastern Romania, solid NH_4NO_3 could form almost all over the year (in both

30 during the cold and the warm seasons) either due to the very complex chemical composition of the collected particles or due to abundant contribution of organic carbon to the particles mass concentration (Dougle et al., 1998). Formation of NH_4NO_3 over the warm seasons has been reported also by Ianniello et al. (2011) but under different conditions. For deliquesced particles there is suggestion that most of the fine particulate NO_3^- can exist as an internal mixture with SO_4^{2-} , and also that HNO_3 can easily be absorbed into the droplets (Huang et al., 2010). In specific circumstances, the fine particulate NO_3^- can



be formed from HNO_3 and NH_3 through heterogeneous reactions on fully neutralized fine particulate SO_4^{2-} , which is abundantly present in an urban area (Stockwell et al., 2000). However, in the present work, during the cold seasons, in the $\text{PM}_{2.5}$ fraction a statistically significant correlation between SO_4^{2-} and NO_3^- was observed ($r = 0.91$, $p < 0.001$, at the 99.9 % confidence level). High concentrations of NO_3^- were found at high levels of RH and SO_4^{2-} concentrations were high over the entire range of RH values. Significant correlation was observed between NO_3^- and RH ($r = 0.84$, $p < 0.001$, at the 99.9 % confidence level) but that between sulfate and RH was not statistically significant ($r = 0.44$, $p = 0.177$). These results can be interpreted as nitrate being produced on pre-existing sulfate aerosols, which could provide sufficient surface area and aerosol water content for the heterogeneous reactions to occur. Although, formation of fine particulate NO_3^- was suggested to occur via reaction (R2), in the previously presented situations and especially at high RH values, the amounts of the gaseous precursors, such as NH_3 and HNO_3 , are expected to have relatively little influence on the fine particulate NO_3^- formation (Markovic et al., 2011).

As for particulate NH_4Cl this is known as usually showing a volatility which is 2–3 times higher than that of NH_4NO_3 (HCl is more volatile than HNO_3) and at humidity lower than 75–85 % the particulate NH_4Cl exists in the solid phase in equilibrium with the gaseous products (Ianniello et al., 2011 and references therein). During the cold seasons, particulate NH_4^+ (total) showed a statistically significant correlation with particulate Cl^- (Pearson coefficient of 0.73, $p < 0.001$, at the 99.9 % confidence level) but during the warm seasons the correlation was of very poor significance (meteorological parameters might be responsible on this). Moreover, only during the cold seasons significant correlations have been observed between fine particulate Cl^- and SO_4^{2-} (Pearson coefficient of 0.59, $p < 0.001$, at the 95.4 % confidence level) and between fine particulate Cl^- and RH (Pearson coefficient of 0.71, $p = 0.010$, at the 95.4 % confidence level) and, usually, high concentrations of fine particulate Cl^- and SO_4^{2-} were found at high levels of RH (35–83 %). Under these circumstances, in all above presented situations, the amount of the gaseous precursors are believed to present relatively little influence on the formation of fine particulate Cl^- and, if formed, NH_4Cl most probably is generated from HCl and NH_3 through heterogeneous reactions on neutralized sulfate particles. However, in the present work, estimation of free Cl^- allow us suggesting that no Cl^- was available to be bond with other chemical species (i.e., NH_4^+) apart with the alkali or alkaline earth metals, and therefore NH_4Cl in significant concentrations was not expected to be formed (especially over the warm seasons).

3.3 Relative ions contribution in size resolved aerosol particles from Iasi and potential influence of long range transport phenomena on particles size distribution

Figures 8a,b,c,d present, as monthly based averages, the relative contributions of identified and quantified water soluble ions to total detected components in fractions grouped in four stages, i.e., 0.0276–0.0945 μm size range (Fig. 8a), 0.155–0.612 μm size range (Fig. 8b), 0.946–2.39 μm size range (Fig. 8c) and 3.99–9.94 μm size range (Fig. 8d). From details presented in Fig. 8a, for the 0.0276–0.0945 μm size range fraction it is obvious that an important contribution within the total detected components is brought by organic anions identified in the formate, acetate and oxalate form. The presence of such important contribution of organics within this submicron size range may actually indicate a possible important role of organic acids in



secondary organic aerosols formation. Higher values over the warm seasons may suggest an enhancement in the role of biogenic emission sources. Important contributions are brought by particulate SO_4^{2-} , NH_4^+ (total), K^+ and unexpected high HCO_3^- . However, high particulate HCO_3^- is also evident for the $0.946\text{--}2.39\text{ }\mu\text{m}$ size range (Fig. 8c) and $3.99\text{--}9.94\text{ }\mu\text{m}$ size range (Fig. 8d) fractions. The $0.155\text{--}0.612\text{ }\mu\text{m}$ size range (Fig. 8b) fraction seems to be mainly constituted by SO_4^{2-} , NO_3^- and NH_4^+ (total) with very small contributions of all other particulate analyzed ions.

The seasonal variation observed mainly for SO_4^{2-} and NO_3^- might suggest an enhancement of photo-oxidative processes over the warm seasons. The $0.946\text{--}2.39\text{ }\mu\text{m}$ (Fig. 8c) and $3.99\text{--}9.94\text{ }\mu\text{m}$ size range (Fig. 8d) fractions seem to present mainly a non-homogeneous chemical composition and are dominated mainly by HCO_3^- , NO_3^- and organics. However, over the investigated period, among all analyzed chemical species, in the PM_{10} fraction SO_4^{2-} is the most abundant with (26.0 ± 4.3) % contribution, followed by NO_3^- with (26.0 ± 10.7) %, NH_4^+ (total) (15.0 ± 3.4) %, organics (including acetate, formate and oxalate) (12.2 ± 3.7) % and HCO_3^- (10 ± 7.7) %. Similarly, in the $\text{PM}_{2.5}$ fraction SO_4^{2-} is the most abundant with (28.9 ± 5.6) % and it is followed by NO_3^- (19.6 ± 12.1) %, NH_4^+ (total) (16.6 ± 3.2) %, organics (including acetate, formate and oxalate) (11.4 ± 4.0) % and HCO_3^- (8.0 ± 6.8) %. In both the PM_{10} and the $\text{PM}_{2.5}$ fractions, the largest contribution of SO_4^{2-} was observed in June 2016 with (34.6 ± 10.9) % and, respectively, (40.8 ± 11.0) %. During the cold seasons, particulate SO_4^{2-} and NO_3^- contributions to the PM_{10} fraction are of (23.6 ± 2.3) % and respectively, (28.6 ± 4.9) %, while during warm seasons these are of (28.5 ± 4.7) % and, respectively, (10.1 ± 4.8) %. In the $\text{PM}_{2.5}$ fraction, over cold seasons, these contributions are of (25.5 ± 2.9) % and respectively, (30.1 ± 5.8) %, while during warm seasons these are of (32.4 ± 5.6) % and, respectively, (9.2 ± 5.4) %. Wonaschutz et al. (2015) report for Vienna (Austria) NO_3^- contributions of 31.3 % during winter and of 6.9 % during summer.

Particulate Ca^{2+} and HCO_3^- , as dust tracers' ions, brought a significant contribution especially over the warm seasons (e.g., contribution of $\sim 43.8 \pm 11.2$ % in PM_{10} and $\sim 37.8 \pm 12.3$ % in $\text{PM}_{2.5}$ brought by the two ions in August 2016), and such contributions would actually reflect that Ca^{2+} and HCO_3^- mostly originate from soil dust re-suspension during dry seasons. In 2016, in Iasi, north-eastern Romania, spring distinguished as the season with predominant air masses undertaking long range transport phenomenon from S-SE sector and the highest contributions from sea-spray aerosols tracers (i.e., Na^+ and Mg^{2+} , Masiol et al., (2012)) were recorded in April (5.8 % for Na^+ and 0.7 % for Mg^{2+}). Such observations would actually allow us suggesting the presence of sea-spray aerosols from the Black Sea or other marine areas in the size resolved aerosols from Iasi. Although in overall SO_4^{2-} , NO_3^- and NH_4^+ (total) ions (as secondary pollution products) are the most abundant, at the investigated site, organics (including acetate, formate and oxalate) might also bring significant contributions $((17.3 \pm 4.4)$ % in PM_{10} fraction and 18.2 ± 5.1 % in $\text{PM}_{2.5}$ fraction in July 2016, much higher than that reported by Arsene et al., (2011) in Iasi). The difference might reflect either an inversion of the photochemistry taking place at the investigated location or differences in the sampling efficiency between the two studies.

Figures 9a,b,c,d show the size distributions of seasonal averaged mass concentrations for Cl^- , NO_3^- , SO_4^{2-} , NH_4^+ (Fig. 9a,b) and K^+ , Na^+ , Mg^{2+} , Ca^{2+} (Fig. 9c,d) ions in atmospheric aerosols from Iasi, both during the cold and, respectively, the warm seasons. While during the cold seasons NO_3^- , SO_4^{2-} , NH_4^+ and K^+ reside mainly in the fine mode with maxima at $\sim 381\text{ nm}$,



all other ions (i.e., Cl^- , Na^+ , Mg^{2+} , Ca^{2+}) seem to present major contributions in the supermicrone mode (maxima between 1.6–2.39 μm). For Cl^- distribution over the cold seasons clear evidences were obtained about its existence in a bimodal mode. During the warm seasons only SO_4^{2-} and K^+ present clear maxima at 381 nm while all other identified/quantified species have more important contributions in the supermicrone mode. For sulfate, larger modal diameter over the cold than over the warm seasons is most likely due to hygroscopic growth under high RH, and/or due to increased secondary aerosol production, lower temperatures facilitating condensation. Secondary aerosol mass from aqueous-phase reactions may also play a role (Wonaschutz et al., 2015). The maxima observed in the coarse mode could also be explained considering that heterogeneous chemistry occurring on dust particles could also act as a source for some particulate species (Wang et al., 2012).

- While particulate NO_3^- over the cold seasons presented monomodal distributions in the submicron size range (maxima at 381 nm), over the warm seasons this ion presented a second mode with maxima in the 1.60 to 2.39 μm size range. Such a size distribution would allow us suggesting that NO_3^- during the warm seasons is most probably produced by adsorption of HNO_3 on sea salt and soil particles (Park et al., 2004). According to Karydis et al. (2016), particulate NO_3^- is not associated only with NH_4^+ in the fine mode. In particular light-metallic ions, as Ca^{2+} , Mg^{2+} , Na^+ , and K^+ mainly present in the coarse mode, can be associated with NO_3^- and affect its partitioning into the aerosol phase. Dust effects on the distribution of particulate species might include decreasing of NH_4^+ fine-mode and shifting of particulate NO_3^- from the fine- to the coarse-mode (Wang et al., 2012). In addition, the presence of significant fractions of particulate NO_3^- , Cl^- , Mg^{2+} , Ca^{2+} and Na^+ ions in the coarse fraction, might suggest that NO_3^- possibly originates from the reactions of HNO_3 with MgCO_3 , CaCO_3 or NaCl . Similar patterns were identified in Vienna, Austria, (Wonaschutz et al., 2015) and Prague, Czech (Schwarz et al., 2012). Significant amounts of particulate NO_3^- formed through the reaction between HNO_3 with CaCO_3 on soil-derived particles have also been observed and reported (Yao et al., 2003; Sharma et al., 2007). Moreover, sea-salt aerosols may also undergo chemical transformation of NaCl to NaNO_3 during their transport (Schwarz et al., 2012).

- The size distributions of particulate K^+ reflect the existence of one dominant fine mode, which most likely reflects contributions from biomass burning all over the year (Schmidl et al., 2008; Pachon et al., 2013). For both Ca^{2+} and Mg^{2+} ions, clear monomodal mass concentration distributions, with maxima in the 1.6 to 2.39 μm size range, have been observed over the investigated period. Over the warm seasons Ca^{2+} seems to account for $(7.0 \pm 2.9) \%$ of the PM_{10} fraction ($(5.5 \pm 2.9) \%$ of the $\text{PM}_{2.5}$ fraction) while over the cold seasons it accounts for only $(3.0 \pm 0.6) \%$ of the PM_{10} fraction ($(2.2 \pm 0.5) \%$ of the $\text{PM}_{2.5}$ fraction) and these observations indicate that the impact from soil dust re-suspension could be more important during the warm (dried) seasons. Mineral dust may also explain the higher coarse fraction of Mg^{2+} (mineral source of MgCO_3).

Clear evidences have been obtained in the present work about the fact that air mass origin might greatly influence aerosol chemical composition at the investigated site. Wonaschutz et al. (2015) suggested that in Vienna, Austria, air mass origin is the most important factor for bulk PM concentrations, chemical composition of the coarse fraction ($> 1.5 \mu\text{m}$) and the mass size distribution, and less important for chemical composition of the fine fraction ($< 1.5 \mu\text{m}$). Although Iasi is located far



from the Mediterranean or Black Sea, over the warm seasons sea-salt chloride contribution to the aerosol budget in the area is not entirely excluded (Arsene et al., 2011). Moreover, dust particles originating from the Sahara are acknowledged as travelling across the tropical Atlantic Ocean ($10\text{--}90\ \mu\text{g m}^{-3}$) and across the Mediterranean, affecting air quality in southern Europe ($10\text{--}60\ \mu\text{g m}^{-3}$) (Karydis et al., 2016). In the present work, particulate Na^+ and Cl^- ions, as tracers of sea-salt aerosols (Tositti et al., 2014), were mainly observed in sampled events predominated by contributions of air masses arriving in Iasi from S-SE directions. However, one of the most interesting collected event was the one conducted 9th to 11th April in 2016. For this event the PM_{10} fraction mass concentration was as high as $43.9\ \mu\text{g m}^{-3}$, a value which is about two times higher than the average of the total events. This event was actually highly influenced by air masses originating from both the Saharan desert and also from Mediterranean Sea. As shown in Fig. 10a the size distributions of particulate Na^+ , Ca^{2+} , Mg^{2+} , Cl^- ions and mass concentrations present a highly dominating mode with maxima at $2.39\ \mu\text{m}$. For this event (Ca^{2+} , Mg^{2+}) and (Na^+ , Cl^-) pairs showed statistically significant correlations (i.e., $r = 0.94$, $p < 0.001$ and, respectively, $r = 0.85$, $p < 0.001$, at the 99.9 % confidence level) suggesting common contributions from mineral Saharan dust and, respectively, from sea-salt marine aerosols. Moreover, Fig. 10a clearly shows that Na^+ , Ca^{2+} , Mg^{2+} , Cl^- mass concentrations make a very significant contribution to the total aerosol mass in the supermicrone mode with the maxima at $2.39\ \mu\text{m}$.

For April 2016 interesting behaviour was also observed for averaged mass size distributions of particulate NH_4^+ , NO_3^- , SO_4^{2-} and Mg^{2+} ions and mass gravimetrically determined in samples collected at AMOS (Fig. 10b). During this month (highly affected by the atmospheric air masses buoyancy phenomenon, as shown by trajectories analysis for selected events collected in April), while particulate NH_4^+ and SO_4^{2-} were mainly residing in the fine mode with clear maxima at $381\ \text{nm}$, NO_3^- and Mg^{2+} presented also a predominant mode in the fraction with maxima between $1.6\text{--}2.39\ \mu\text{m}$. Such distributions, corroborated with meteorological conditions, would actually suggest possible heterogeneous formation route for SO_4^{2-} (Wang et al., 2012), while for NO_3^- adsorption of HNO_3 on mineral dust and sea salt particles (Karydis et al., 2016) would become more important.

4 Conclusions

The atmospheric concentrations of particulate species including acetate, ($\text{C}_2\text{H}_3\text{O}_2^-$), formate, (HCO_2^-), fluoride, (F^-), chloride, (Cl^-), nitrite, (NO_2^-), nitrate, (NO_3^-), phosphate, (PO_4^{3-}), sulfate, (SO_4^{2-}), oxalate, ($\text{C}_2\text{O}_4^{2-}$), sodium, (Na^+), potassium, (K^+), ammonium, (NH_4^+), magnesium, (Mg^{2+}) and calcium (Ca^{2+}), have been measured in Iasi urban site, north-eastern Romania, over the 2016 year. The measurements were carried out by means of a cascade Dekati Low-Pressure Impactor (DLPI) performing aerosol size classification in 13 specific fractions evenly distributed over the 0.0276 up to $9.94\ \mu\text{m}$ size range.

The entire data set was analyzed such as to investigate the seasonal variations in fine particulate species and meteorological effects, and to examine the contribution of local and regional sources to fine particulate species. ISORROPIA-II



thermodynamic model runs were used to estimate the pH of collected atmospheric particles since on the present data-base it has been proved that this was the best method to analyze particles acidity.

Within the aerosol mass concentration the ionic mass brings contribution as high as 40.6 % with the rest being unaccounted yet. Fine particulate Cl^- , NO_3^- , NH_4^+ and K^+ exhibited clear seasonal variations (with minima during the warm seasons), mainly controlled by corroboration between factors as enhancement in the emission sources, changes in the mixed layer depth and specific meteorological conditions (e.g., higher RH values prevailing during cold seasons). Fine particulate SO_4^{2-} did not show much variation with respect to seasons. Particulate NH_4^+ and NO_3^- measured concentration in fine mode ($\text{PM}_{2.5}$) aerosols were found to be in reasonable good agreement with modelled values for the cold seasons but not for the warm seasons, an observation reflecting actually the susceptibility of NH_4NO_3 aerosols to be lost due to volatility.

Clear evidences have been obtained for the fact that in Iasi, north-eastern Romania, NH_4^+ in $\text{PM}_{2.5}$ was primarily associated with SO_4^{2-} and NO_3^- . However, indirect ISORROPIA-II estimations showed that the atmosphere in Iasi, north-eastern Romania, might be ammonia-rich during both the cold and warm seasons, such as enough NH_3 to be present to neutralize H_2SO_4 , HNO_3 and HCl acidic components and to generate fine particulate ammonium salts, in the form of $(\text{NH}_4)_2\text{SO}_4$, NH_4NO_3 and NH_4Cl . Significant amounts of fine particulate NO_3^- have been found mainly during the cold seasons such as to promote NH_4NO_3 formation. The presence of eventual large amounts of NH_3 , the domination of $(\text{NH}_4)_2\text{SO}_4$ over NH_4NO_3 and NH_4Cl , the high relative humidity conditions (highly prevailing over the cold seasons) dissolving probably a significant fraction of atmospheric HNO_3 and NH_3 , are among the most important driving forces enhancing fine particulate NO_3^- and NH_4^+ distribution in the atmosphere of Iasi, north-eastern Romania.

Most probably in Iasi, north-eastern Romania, gaseous NH_3 is not acting as the sole precursor of NH_4^+ formation, but it exerts an important role on NO_3^- and eventually Cl^- formation in $\text{PM}_{2.5}$ via neutralization process. The chemical composition data-base in $\text{PM}_{2.5}$ (and PM_{10}), combined with predictions from the thermodynamic model ISORROPIA-II in the forward mode, metastable, allow us suggesting that at the investigated site, most probably NH_3 was present in sufficiently high concentration at most time such as to promote fine particle acidity neutralisation both during the cold and during the warm seasons. Although it is already known that running ISORROPIA-II in the forward mode, but with only aerosol concentrations as input may result in a bias in predicted pH due to repartitioning of ammonia in the model, this approach was the single one helping to interpret the obtained results in a more trustful way.

Over the warm seasons ~ 35 % of the total analyzed samples presented pH values in the very strong acidity fraction (0–3 pH units range) while over the cold seasons the contribution in this pH range was of ~ 43 %. However, while during the warm seasons ~ 24–25 % of the acidic samples were with pH values in the 1–2 range (reflecting mainly contributions from very strong inorganic acids), over the cold seasons an increase to ~ 40 %, brought by the 1–3 pH range, would reflect possible contributions from other acidic type species (i.e., organics), changes in aerosols acidity impacting actually the gas–particle partitioning of semi-volatile organic acids.



Acknowledgements

The authors acknowledge the financial support provided by UEFISCDI within the PN-III-P4-ID-PCE-2016-0299 (AI-FORECAST), PN-II-PCE-2011-3-0471 (EVOLUTION-AIR) and PN-II-RU-TE-2014-4-2461 (SOS-AROMATIC) projects. European Union's Horizon 2020 research and innovation programme through the EUROCHAMP-2020 Infrastructure Activity under grant agreement No 730997 is also gratefully acknowledged. The authors acknowledge also the NOAA Air Resources Laboratory (ARL) for the provision of the HYSPLIT transport and dispersion model and/or READY website (<http://www.ready.noaa.gov>) used in this publication.

References

- Adams, P. J., Seinfeld, J. H., and Koch, D. M.: Global concentration of tropospheric sulphate, nitrate and ammonium aerosol simulated in a general circulation model, *J. Geophys. Res.*, 104, 13791–13823, doi:10.1029/1999JD900083, 1999.
- Akagi, S. K., Yokelson, R. J., Wiedinmyer, C., Alvarado, M. J., Reid, J. S., Karl, T., Crounse, J. D., and Wennberg, P. O.: Emission factors for open and domestic biomass burning for use in atmospheric models, *Atmos. Chem. Phys.*, 11, 4039–4072, doi:10.5194/acp-11-4039-2011, 2011.
- Alastuey, A., Querol, X., Rodríguez, S., Plana, F., Lopez-Soler, A., Ruiz, C., and Mantilla, E.: Monitoring of atmospheric particulate matter around sources of inorganic secondary inorganic aerosol, *Atmos. Environ.*, 38, 4979–4992, doi:10.1016/j.atmosenv.2004.06.026, 2004.
- Alastuey, A., Querol, X., Aas, W., Lucarelli, F., Perez, N., Moreno, T., Cavalli, F., Areskou, H., Balan, V., Catrambone, M., Ceburnis, D., Cerro, J. C., Conil, S., Gevorgyan, L., Hueglin, C., Imre, K., Jaffrezo, J. L., Leeson, S. R., Mihalopoulos, N., Mitosinkova, M., O'Dowd, C. D., Pey, J., Putaud, J. P., Riffault, V., Ripoll, A., Sciare, J., Sellegri, K., Spindler, G., Yttri, and K. E.: Geochemistry of PM₁₀ over Europe during the EMEP intensive measurement periods in summer 2012 and winter 2013, *Atmos. Chem. Phys.*, 16, 6107–6129, doi:10.5194/acp-16-6107-2016, 2016.
- Aneja, V. P., Chauhan, J. P., and Walker, J. T.: Characterization of atmospheric ammonia emissions from swine waste storage and treatment lagoons, *J. Geophys. Res.*, 105, 11535–11545, doi:10.1029/2000JD900066, 2000.
- Arsene, C., Olariu, R. I., and Mihalopoulos, N.: Chemical composition of rainwater in the north-eastern Romania, Iasi region (2003–2006), *Atmos. Environ.*, 41, 9452–9467, doi:10.1016/j.atmosenv.2007.08.046, 2007.
- Arsene, C., Olariu, R. I., Zarmas, P., Kanakidou, M., and Mihalopoulos, N.: Ion composition of coarse and fine particles in Iasi, north-eastern Romania. Implications for aerosols chemistry in the area, *Atmos. Environ.*, 45, 906–916, doi:10.1029/2000JD900066, 2011.
- Athanasopoulou, E., Tombrou, M., Pandis, S. N., and Russell, A. G.: The role of sea-salt emissions and heterogeneous chemistry in the air quality of polluted coastal areas, *Atmos. Chem. Phys.*, 8, 5755–5769, doi:10.5194/acp-8-5755-2008, 2008.



- Bacarella, A. L., Grunwald, E., Marshall, H. P., and Purlee, E. L.: The potentiometric measurement of acid dissociation constants and pH in the system methanol-water. pK_a values for carboxylic acids and anilinium ions, *J. Org. Chem.*, 20, 747–762, doi:10.1021/jo01124a007, 1955.
- Backes, A. M., Aulinger, A., Bieser, J., Matthias, V., and Quante, M.: Ammonia emissions in Europe, part II: How ammonia
5 emission abatement strategies affect secondary aerosols, *Atmos. Environ.*, 126, 153–161, doi:10.1016/j.atmosenv.2015.11.039, 2016.
- Bardouki, H., Liakakou, H., Economou, C., Sciare, J., Smolik, J., Zdimal, V., Eleftheriadis, K., Lazaridis, M., Dye, C., and Mihalopoulos, N.: Chemical composition of size-resolved atmospheric aerosols in the eastern Mediterranean during summer and winter, *Atmos. Environ.*, 37, 195–208, doi: 10.1016/S1352-2310(02)00859-2, 2003.
- 10 Behera, S. N. and Sharma, M.: Transformation of atmospheric ammonia and acid gases into components of $PM_{2.5}$: an environmental chamber study, *Environ. Sci. Pollut. Res.*, 19, 1187–1197, doi:10.4209/aaqr.2012.11.0328, 2012.
- Behera, S. N., Betha, R., and Balasubramanian, R.: Insights into chemical coupling among acidic gases, ammonia and secondary inorganic aerosols, *Aerosol Air Qual. Res.*, 13, 1282–1296, doi:10.1007/s11356-011-0635-9, 2013.
- Bressi, M., Sciare, J., Ghersi, V., Bonnaire, N., Nicolas, J. B., Petit, J. E., Moukhtar, S., Rosso, A., Mihalopoulos, N., and
15 Feron, A.: A one-year comprehensive chemical characterisation of fine aerosol ($PM_{2.5}$) at urban, suburban and rural background sites in the region of Paris (France), *Atmos. Chem. Phys.*, 13, 7825–7844, doi:10.5194/acp-13-7825-2013, 2013.
- Brook, R. D.: Cardiovascular effects of air pollution, *Clin. Sci.*, 115, 175–187, doi: doi: 10.1042/CS20070444, 2008.
- Christian, T. J., Yokelson, R. J., Cardenas, B., Molina, L. T., Engling, G., and Hsu, S. C.: Trace gas and particle emissions from domestic and industrial biofuel use and garbage burning in central Mexico, *Atmos. Chem. Phys.*, 10, 565–584,
20 doi:10.5194/acp-10-565-2010, 2010.
- Clegg, S. L., Brimblecombe, P., and Wexler, A. S.: Thermodynamic model of the system $H^+ - NH_4^+ - SO_4^{2-} - NO_3^- - H_2O$ at tropospheric temperatures, *J. Phys. Chem. A*, 102, 2137–2154, doi:10.1021/jp973042r, 1998.
- Cziczo, D. J., Nowak, J. B., Hu, J. H., and Abbatt, J. P. D.: Infrared spectroscopy of model tropospheric aerosols as a function of relative humidity: observation of deliquescence and crystallization, *J. Geophys. Res.*, 102, 18843–18850,
25 doi:10.1029/97JD01361, 1997.
- Directive 2008/50/EC of the European Parliament and of the Council of 21 May 2008 on ambient air quality and cleaner air for Europe, *Official Journal L* 152, 11/06/2008, pp. 0001–0044, 2008.
- Dominici, F., Peng, D. K., Bell, M. L., Pham, L., McDermott, A., Zeger, S. L., and Samet, J. M.: Fine particulate air pollution and hospital admission for cardiovascular and respiratory diseases, *JAMA*, 295, 1127–1134,
30 doi:10.1001/jama.295.10.1127, 2006.
- Dougle P. G., Veefkind J. P., and ten Brink, H. M.: Crystallisation of mixtures of ammonium nitrate, ammonium sulphate and soot, *J. Aerosol Sci.*, 29, 3, 375–386, doi:10.1016/S0021-8502(97)10003-9, 1998.
- EEA Report, European Environment Agency Report, Air quality in Europe-2015 report, ISSN 1977–8449, Report No. 5, 2015.



- Fang, T., Guo, H., Zeng, L., Verma, V., Nenes, A., and Weber, R. J.: Highly acidic ambient particles, soluble metals, and oxidative potential: A link between sulfate and aerosol toxicity, *Environ. Sci. Technol.*, 51, 2611–2620, doi:10.1021/acs.est.6b06151, 2017.
- Fountoukis, C. and Nenes, A.: ISORROPIA II: a computationally efficient thermodynamic equilibrium model for K^+ – Ca^{2+} – Mg^{2+} – NH_4^+ – Na^+ – SO_4^{2-} – NO_3^- – Cl^- , and H_2O aerosols, *Atmos. Chem. Phys.*, 7, 4639–4659, doi:10.5194/acp-7-4639-2007, 2007.
- 5 Fountoukis, C., Nenes, A., Sullivan, A., Weber, R., Van Reken, T., Fischer, M., Matias, E., Moya, M., Farmer, D., and Cohen, R. C.: Thermodynamic characterization of Mexico City aerosol during MILAGRO 2006, *Atmos. Chem. Phys.*, 9, 2141–2156, doi:10.5194/acp-9-2141-2009, 2009.
- 10 Freney, E., Sellegri, K., Canonaco, F., Colomb, A., Borbon, A., Michoud, V., Doussin, J. F., Crumeyrolle, S., Amarouche, N., Pichon, J. M., Bourianne, T., Gomes, L., Prevot, A. S. H., Beekmann, M., and Schwarzenboeck, A.: Characterizing the impact of urban emissions on regional aerosol particles: airborne measurements during the MEGAPOLI experiment, *Atmos. Chem. Phys.*, 14, 1397–1412, doi:10.5194/acp-14-1397-2014, 2014.
- Gerasopoulos, E., Koulouri, E., Kalivitis, N., Kouvarakis, G., Sarrikoski, S., Makela, T., Hillamo, R., and Mihalopoulos, N.: Size-segregated mass distribution of aerosols near Eastern Mediterranean: seasonal variability and comparison with AERONET columnar size-distributions, *Atmos. Chem. Phys.*, 7, 2551–2561, doi:10.5194/acp-7-2551-2007, 2007.
- 15 Guo, H., Xu, L., Bougiatioti, A., Cerully, K. M., Capps, S. L., Hite, J. R., Carlton, A. G., Lee, S. H., Bergin, M. H., Ng, N. L., Nenes, A., and Weber, R. J.: Particle water and pH in the southeastern United States, *Atmos. Chem. Phys.*, 15, 5211–5228, doi: 10.5194/acp-15-5211-2015, 2015.
- 20 Guo, H., Sullivan, A. P., Campuzano-Jost, P., Schroder, J. C., Lopez-Hilfiker, F. D., Dibb, J. E., Jimenez, J. L., Thornton, J. A., Brown, S. S., Nenes, A., and Weber, R. J.: Fine particle pH and the partitioning of nitric acid during winter in the northeastern United States, *J. Geophys. Res.: Atmos.*, 121, 10355–10376, doi: 10.1002/2016JD025311, 2016.
- Harrison, R. M. and Kitto, A. M. N.: Estimation of the rate constant for the reaction of acid sulfate aerosol with NH_3 gas from atmospheric measurements, *J. Atmos. Chem.*, 15, 133–143, doi:10.1007/BF00053755, 1992.
- 25 Hasheminassab, S., Daher, N., Saffari, A., Wang, D., Ostro, B. D., and Sioutas, C.: Spatial and temporal variability of sources of ambient fine particulate matter ($PM_{2.5}$) in California, *Atmos. Chem. Phys.*, 14, 12085–12097, doi:10.5194/acp-14-12085-2014, 2014.
- Hennigan, C. J., Izumi, J., Sullivan, A. P., Weber, R. J., and Nenes, A.: A critical evaluation of proxy methods used to estimate the acidity of atmospheric particles, *Atmos. Chem. Phys.*, 15, 2775–2790, doi:10.5194/acp-15-2775-2015, 2015.
- 30 Hitznerberger, R., Ctyroky, P., Berner, A., Tursic, J., Podkrajsek, B., and Grgic, I.: Size distribution of black (BC) and total carbon (TC) in Vienna and Ljubljana, *Chemosphere*, 65, 2106–2113, doi:10.1016/j.chemosphere.2006.06.042, 2006.
- Holton, J. R.: *An Introduction to Dynamic Meteorology*, 4th ed., Academic Press, New York, 1979.
- Huang, X. F., He, L. Y., Hu, M., Canagaratna, M. R., Sun, Y., Zhang, Q., Zhu, T., Xue, L., Zeng, L. W., Liu, X. G., Zhang, Y. H., Jayne, J. T., Ng, N. L., and Worsnop, D. R.: Highly time-resolved chemical characterization of atmospheric



- submicron particles during 2008 Beijing Olympic Games using an Aerodyne High-Resolution Aerosol Mass Spectrometer, *Atmos. Chem. Phys.*, 10, 8933–8945, doi:10.5194/acp-10-8933-2010, 2010.
- Ianniello, A., Spataro, F., Esposito, G., Allegrini, I., Rantica, E., Ancora, M. P., Hu, M., and Zhu, T.: Occurrence of gas phase ammonia in the area of Beijing (China), *Atmos. Chem. Phys.*, 10, 9487–9503, doi:10.5194/acp-10-9487-2010, 2010.
- 5 Ianniello, A., Spataro, F., Esposito, G., Allegrini, I., Hu, M., and Zhu, T.: Chemical characteristics of inorganic ammonium salts in PM_{2.5} in the atmosphere of Beijing (China), *Atmos. Chem. Phys.*, 11, 10803–10822, doi:10.5194/acp-11-10803-2011, 2011.
- Ichim, L., Vlaicu, M., Draxineanu, A., and Alexandru, C.: Populatia Romaniei pe localitati la 1 Ianuarie 2016, in INS 2016, Iagar, E.M., Pisica, S., Baltateanu, L., (eds.), ISSN: 2066–2181, Institutul National de Statistica, Romania, pp. 130, 2016.
- 10 IPCC, 2013: Summary for Policymakers, in: *Climate Change 2013: The Physical Science Basis. Contribution of Working Group I to the Fifth Assessment Report of the Intergovernmental Panel on Climate Change* [Stocker, T. F., Qin, D., Plattner, G. K., Tignor, M., Allen, S. K., Boschung, J., Nauels, A., Xia, Y., Bex, V., Midgley P., M., (eds.)], Cambridge University Press, Cambridge, United Kingdom and New York, NY, USA, pp. 1–30, doi:10.1017/CBO9781107415324.004, 2013.
- ISORROPIA Main Page: <http://isorroopia.eas.gatech.edu/>, last access: 11 July 2017.
- 15 James, P. M.: An objective classification method for Hess and Brezowsky Grosswetterlagen over Europe, *Theor. Appl. Climatol.*, 88, 17–42, doi:10.1007/s00704-006-0239-3, 2007.
- Jang, M., Czoschke, N. M., Lee, S., and Kamens, R. M.: Heterogeneous atmospheric aerosol production by acid-catalyzed particle-phase reactions, *Science*, 298, 814–817, doi:10.1126/science.1075798, 2002.
- Kadowaki, S.: On the nature of the atmospheric oxidation processes of SO₂ to sulphate and of NO₂ to nitrate on the basis of
- 20 diurnal variations of sulphate, nitrate, and other pollutants in an urban area, *Environ. Sci. Technol.*, 20, 1249–1253, doi:10.1021/es00154a009, 1986.
- Kai, Z., Yuesi, W., Tianxue, W., Yousef, M., and Frank, M.: Properties of nitrate, sulfate and ammonium in typical polluted atmospheric aerosols (PM₁₀) in Beijing, *Atmos. Res.*, 84, 67–77, doi:10.1016/j.atmosres.2006.05.004, 2007.
- Karydis, V. A., Tsimpidi, A. P., Lei, W., Molina, L. T., and Pandis, S. N.: Formation of semivolatile inorganic aerosols in
- 25 the Mexico City Metropolitan Area during the MILAGRO campaign, *Atmos. Chem. Phys.*, 11, 13305–13323, doi:10.5194/acp-11-13305-2011, 2011.
- Karydis, V. A., Tsimpidi, A. P., Pozzer, A., Astitha, M., and Lelieveld, J.: Effects of mineral dust on global atmospheric nitrate concentrations, *Atmos. Chem. Phys.*, 16, 1491–1509, doi:10.5194/acp-16-1491-2016, 2016.
- Keene, W. C., Pszenny, A. A. P., Maben, J. R., Stevenson, E., and Wall, A.: Closure evaluation of size-resolved aerosol pH
- 30 in the New England coastal atmosphere during summer, *J. Geophys. Res.*, 109, D23307, doi:10.1029/2004JD004801, 2004.
- Kocak, M., Mihalopoulos, N., and Kubilay, N.: Contributions of natural sources to high PM₁₀ and PM_{2.5} events in the eastern Mediterranean, *Atmos. Environ.*, 41, 3806–3818, doi:10.1016/j.atmosenv.2007.01.009, 2007.
- Laongsri, B. and Harrison, R. M.: Atmospheric behaviour of particulate oxalate at UK urban background and rural sites, *Atmos. Environ.*, 71, 319–326, doi:10.1016/j.atmosenv.2013.02.015, 2013.



- Lelieveld, J., Evans, J. S., Fnais, M., Giannadaki, D., and Pozzer, A.: The contribution of outdoor air pollution sources to premature mortality on a global scale, *Nature*, 525, 367–371, doi:10.1038/nature15371, 2015.
- Li, W., Shi, Z., Zhang, D., Zhang, X., Li, P., Feng, Q., Yuan, Q., and Wang, W.: Haze particles over a coal-burning region in the China Loess Plateau in winter: three flight missions in December 2010, *J. Geophys. Res.*, 117, D12306, doi:10.1029/2012JD017720, 2012.
- Li, T. C., Yuan, C. S., Lo, K. C., Hung, C. H., Wu, S. P., and Tong, C.: Seasonal variation and chemical characteristics of atmospheric particles at Three Islands in the Taiwan Strait, *Aerosol Air Qual. Res.*, 15, 2277–2290, doi:10.4209/aaqr.2015.03.0153, 2015.
- Markovic, M. Z., Hayden, K. L., Murphy, J. G., Makar, P. A., Ellis, R. A., Chang, R. Y. W., Slowik, J. G., Mihele, C., and Brook, J.: The effect of meteorological and chemical factors on the agreement between observations and predictions of fine aerosol composition in southwestern Ontario during BAQS-Met, *Atmos. Chem. Phys.*, 11, 3195–3210, doi:10.5194/acp-11-3195-2011, 2011.
- Masiol, M., Squizzato, S., Ceccato, D., Rampazzo, G., and Pavoni, B.: Determining the influence of different atmospheric circulation patterns on PM₁₀ chemical composition in a source apportionment study, *Atmos. Environ.*, 63, 117–124, doi:10.1016/j.atmosenv.2012.09.025, 2012.
- Matsumoto, K. and Tanaka, H.: Formation and dissociation of atmospheric particulate nitrate and chloride: an approach based on phase equilibrium, *Atmos. Environ.*, 30, 639–648, doi:10.1016/1352-2310(95)00290-1, 1996.
- Meng, Z. Y., Seinfeld, J. H., Saxena, P., and Kim, Y. P.: Atmospheric gas - aerosol equilibrium IV. Thermodynamics of carbonates, *Aerosol Sci. Technol.*, 23, 131–154, doi:10.1080/02786829508965300, 1995.
- Meng, Z. Y., Lin, W. L., Jiang, X. M., Yan, P., Wang, Y., Zhang, Y. M., Jia, X. F., and Yu, X. L.: Characteristics of atmospheric ammonia over Beijing, China, *Atmos. Chem. Phys.*, 11, 6139–6151, doi:10.5194/acp-11-6139-2011, 2011.
- Meskhidze, N., Chameides, W. L., Nenes, A., and Chen, G.: Iron mobilization in mineral dust: Can anthropogenic SO₂ emissions affect ocean productivity?, *Geophys. Res. Lett.*, 30, 2085, doi: 10.1029/2003GL018035, 2003.
- Metzger, S., Mihalopoulos, N., and Lelieveld, J.: Importance of mineral cations and organics in gas-aerosol partitioning of reactive nitrogen compounds: case study based on MINOS results, *Atmos. Chem. Phys.*, 6, 2549–2567, doi:10.5194/acp-6-2549-2006, 2006.
- Moya, M., Pandis, S. N., and Jacobson, M. J.: Is the size distribution of urban aerosols determined by thermodynamic equilibrium? An application to Southern California, *Atmos. Environ.*, 36, 2349–2365, doi: 10.1016/S1352-2310(01)00549-0, 2002.
- Nenes, A., Pilinis, C., and Pandis, S. N.: Continued development and testing of a new thermodynamic aerosol module for urban and regional air quality models, *Atmos. Environ.*, 33, 1553–1560, doi:10.1016/S1352-2310(98)00352-5, 1999.
- Nowak, J. B., Huey, L. G., Russell, A. G., Tian, D., Neuman, J. A., Orsini, D., Sjostedt, S. J., Sullivan, A. P., Tanner, D. J., Weber, R. J., Nenes, A., Edgerton, E., and Fehsenfeld, F. C.: Analysis of urban gas phase ammonia measurements from the



- 2002 Atlanta Aerosol Nucleation and Real-Time Characterization Experiment (ANARChE), *J. Geophys. Res.*, 111, D17308, doi: 10.1029/2006JD007113, 2006.
- Olariu, R. I., Vione, D., Grinberg, N., and Arsene C.: Applications of liquid chromatographic techniques in the chemical characterization of atmospheric aerosols, *J. Liq. Chromatogr. Related Technol.*, 38, 322–348, doi:10.1080/10826076.2014.941256, 2015.
- 5 Ostro, B., Malig, B., Broadwin, R., Basu, R., Gold, E. B., Bromberger, J. T., Derby, C., Feinstein, S., Greendale, G. A., Jackson, E. A., Kravitz, H. M., Matthews, K. A., Sternfeld, B., Tomey, K., Green, R. R., and Green, R.: Chronic PM_{2.5} exposure and inflammation: determining sensitive subgroups in mid-life women, *Environ. Res.*, 132, 168–175, doi: 10.1016/j.envres.2014.03.042, 2014.
- 10 Pachon, J. E., Weber, R. J., Zhang, X., Mulholland, J. A., and Russell, A. G.: Revising the use of potassium (K) in the source apportionment of PM_{2.5}, *Atmos. Pollut. Res.*, 4, 14–21, doi: 10.5094/APR.2013.002, 2013.
- Pandolfi, M., Amato, F., Reche, C., Alastuey, A., Otjes, R. P., Blom, M. J., and Querol, X.: Summer ammonia measurements in a densely populated Mediterranean city, *Atmos. Chem. Phys.*, 12, 7557–7575, doi:10.5194/acp-12-7557-2012, 2012.
- Park, R. J., Jacob, D. J., Field, B. D., Yantosca, R. M., and Chin, M.: Natural and transboundary pollution influences on sulfate-nitrate-ammonium aerosols in the United States: implications for policy, *J. Geophys. Res.*, 109, D15204, doi:10.1029/2003JD004473, 2004.
- 15 Pathak, R. K., Wu, W. S., and Wang, T.: Summertime PM_{2.5} ionic species in four major cities of China: nitrate formation in an ammonia-deficient atmosphere, *Atmos. Chem. Phys.*, 9, 1711–1722, doi: 10.1016/S1352-2310(98)00352-5, 2009.
- Pathak, R. K., Wang, T., and Wu, W. S.: Nighttime enhancement of PM_{2.5} nitrate in ammonia-poor atmospheric conditions in Beijing and Shanghai: Plausible contributions of heterogeneous hydrolysis of N₂O₅ and HNO₃ partitioning, *Atmos. Environ.*, 45, 1183–1191, doi:10.1016/j.atmosenv.2010.09.003, 2011.
- Pope, C. A., Burnett, R. T., Thurston, G. D., Thun, M. J., Calle, E. E., Krewski, D., and Godleski, J. J.: Cardiovascular mortality and long-term exposure to particulate air pollution: epidemiological evidence of general pathophysiological pathways of disease, *Circulation*, 109, 71–77, doi: 10.1161/01.CIR.0000108927.80044.7F, 2004.
- 25 Prinn, R. G.: The cleansing capacity of atmosphere, *Annu. Rev. Environ. Resour.*, 28, 29, doi:10.1146/annurev.energy.28.011503.163425, 2003.
- Querol, X., Alastuey, A., Ruiz, C. R., Artinano, B., Hansson, H. C., Harrison, R. M., Buringh, E., ten Brink, H. M., Lutz, M., Bruckmann, P., Straehl, P., and Schneider, J.: Speciation and origin of PM₁₀ and PM_{2.5} in selected European cities, *Atmos. Environ.*, 38, 6547–6555, doi:10.1016/j.atmosenv.2004.08.037, 2004.
- 30 Ramanathan, V., Crutzen, P. J., Kiehl, J. T., and Rosenfeld, D.: Aerosols, climate, and the hydrological cycle, *Science*, 294, 2119–2124, doi:10.1126/science.1064034, 2001.
- Ravishankara, A. R.: Heterogeneous and multiphase chemistry in the troposphere, *Science*, 276, 1058–1065, doi:10.1126/science.276.5315.1058, 1997.



- Rolph, G., Stein, A., and Stunder, B.: Real-time Environmental Applications and Display sYstem: READY, *Environmental Modelling and Software*, 95, 210–228, doi:10.1016/j.envsoft.2017.06.025, 2017.
- Sandrini, S., Van Pinxteren, D., Giulianelli, L., Herrmann, H., Poulain, L., Facchini, C. M., Gilardoni, S., Rinaldi, M., Paglione, M., Turpin, B. J., Pollini, F., Bucci, S., Zanca, N., and Decesari, S.: Size-resolved aerosol composition at an urban
5 and a rural site in the Po Valley in summertime: Implications for secondary aerosol formation, *Atmos. Chem. Phys.*, 16 (17), 10879–10897, doi:10.5194/acp-16-10879-2016, 2016.
- Schmidl, C., Marr, I. L., Caseiro, A., Kotianova, P., Berner, A., Bauer, H., Kasper-Giebla A., and Puxbaum, H.: Chemical characterisation of fine particle emissions from wood stove combustion of common woods growing in mid-European Alpine regions, *Atmos. Environ.*, 42, 126–141, doi:10.1016/j.atmosenv.2007.09.028, 2008.
- 10 Schwarz, J., Chi, X., Maenhaut, W., Civis, M., Hovorka, J., and Smolik, J.: Elemental and organic carbon in atmospheric aerosols at downtown and suburban sites in Prague, *Atmos. Res.*, 90, 287–302, doi:10.1016/j.atmosres.2008.05.006, 2008.
- Schwarz, J., Stefancova, L., Maenhaut, W., Smolik, J., and Zdimal, V.: Mass and chemically speciated size distribution of Prague aerosol using an aerosol dryer - The influence of air mass origin, *Sci Total. Environ.*, 437, 348–362, doi:10.1016/j.scitotenv.2012.07.050, 2012.
- 15 Seinfeld, J. H. and Pandis, S. N.: *Atmospheric Chemistry and Physics: From Air Pollution to Climate Change*, Wiley: New York, 1998.
- Sharma, M., Kishore, S., Tripathi, S. N., and Behera, S. N.: Role of atmospheric ammonia in the secondary particulate matter: a study at Kanpur, India, *J. Atmos. Chem.*, 58, 1–17, doi:10.1007/s10874-007-9074-x, 2007.
- Shon, Z., Ghosh, S., Kim, K., Song, S., Jung, K., and Kim, N.: Analysis of water-soluble ions and their precursor gases over
20 diurnal cycle, *Atmos. Res.*, 132–133, 309–321, doi:10.1016/j.atmosres.2013.06.003, 2013.
- Sicard, P., Lesne, O., Alexandre, N., Mangin, A., and Collomp, R.: Air quality trends and potential health effects e development of an aggregate risk index, *Atmos. Environ.*, 45, 5, 1145–1153, doi:10.1016/j.atmosenv.2010.12.052, 2011.
- Stein, A. F., Draxler, R. R., Rolph, G. D., Stunder, B. J. B., Cohen, M. D., and Ngan, F.: NOAA's HYSPLIT atmospheric transport and dispersion modeling system, *Bull. Am. Meteorol. Soc.*, 96, 2059–2077, doi:10.1175/BAMS-D-14-00110.1,
25 2015.
- Stelson, A. W. and Seinfeld, J. H.: Relative humidity and pH dependence of the vapour pressure of ammonium nitrate-nitric acid solutions at 25 °C, *Atmos. Environ.*, 16, 993–1000, doi:10.1016/0004-6981(82)90185-8, 1982.
- Stockwell, W. R. and Calvert, J. G.: The mechanism of the HO-SO₂ reaction, *Atmos. Environ.*, 17, 2231–2235, doi:10.1016/0004-6981(83)90220-2, 1983.
- 30 Stockwell, W. R., Watson, J. G., Robinson, N. F., Steiner, W., and Sylte, W.: The ammonium nitrate particle equivalent of NO_x emissions for wintertime conditions in Central California's San Joaquin Valley, *Atmos. Environ.*, 34, 4711–4717, doi:10.1016/S1352-2310(00)00148-5, 2000.



- Sun, J., Zhang, Q., Canagaratna, M. R., Zhang, Y., Ng, N. L., Sun, Y., Jayne, J. T., Zhang, X., Zhang, X., and Worsnop, D. R.: Highly time- and size-resolved characterization of submicron aerosol particles in Beijing using an Aerodyne Aerosol Mass Spectrometer, *Atmos. Environ.*, 44, 131–140, doi:10.1016/j.atmosenv.2009.03.020, 2010.
- Sutton, M. A., Howard, C. M., Erisman, J. W., Billen, G., Bleeker, A., Grennfelt, P., van Grinsven, H., and Grizzetti, B.: The European Nitrogen Assessment: Sources, Effects and Policy Perspectives, Cambridge University Press, 2011.
- 5 Tolis, E. I., Saraga, D. E., Lytra, M. K., Papathanasiou, A. C., Bougaidis, P. N., Prekas-Patronakis, O. E., Ioannidis, I. I., and Bartzis, J. G.: Concentration and chemical composition of PM_{2.5} for a one-year period at Thessaloniki, Greece: a comparison between city and port area, *Atmos. Environ.*, 113, 197–207, doi:10.1016/j.atmosenv.2015.05.014, 2015.
- Tositti, L., Brattich, E., Masiol, M., Baldacci, D., Ceccato, D., Parmeggiani, S., Stracquadanio, M., and Zappoli, S.: Source apportionment of particulate matter in a large city of southeastern Po Valley (Bologna, Italy), *Environ. Sci. Pollut. Res.*, 21, 872–890, doi:10.1007/s11356-013-1911-7, 2014.
- 10 Trebs, I., Metzger, S., Meixner, F. X., Helas, G., Hoffer, A., Andreae, M. O., Moura, M. A. L., da Silva Jr., R. S., Rudich, Y., Falkovich, A. H., Artaxo, P., and Slanina, J.: The NH₄⁺–NO₃[–]–Cl[–]–SO₄^{2–}–H₂O aerosol system and its gas phase precursors at a pasture site in the Amazon Basin: How relevant are mineral cations and soluble organic acids?, *J. Geophys. Res.*, 110, D07303, doi:10.1029/2004JD005478, 2005.
- 15 Tsai, Y. I. and Cheng, M. T.: Visibility and aerosol chemical compositions near the coastal area in Central Taiwan, *Sci. Total Environ.*, 231, 37–51, doi:10.1016/S0048-9697(99)00093-5, 1999.
- Tursic, J., Podkrajsek, B., Grgic, I., Ctyroky, P., Berner, A., Dusek, U., and Hitzengerger, R.: Chemical composition and hygroscopic properties of size-segregated aerosol particles collected at the Adriatic coast of Slovenia, *Chemosphere*, 63, 1193–1202, doi:10.1016/j.chemosphere.2005.08.040, 2006.
- 20 Utsunomiya, A. and Wakamatsu, S.: Temperature and humidity dependence on aerosol composition in the northern Kyushu, Japan, *Atmos. Environ.*, 30, 2379–2386, doi:10.1016/1352-2310(95)00350-9, 1996.
- Voutsas, D., Samara, C., Manoli, E., Lazarou, D., and Tzoumaka, P.: Ionic composition of PM_{2.5} at urban sites of northern Greece: secondary inorganic aerosol formation, *Environ. Sci. Pollut. Res.*, 21, 4995–5006, doi:10.1007/s11356-013-2445-8, 2014.
- 25 Wang, Y., Zhuang, G., Tang, A., Yuan, H., Sun, Y., Chen, Sh., and Zheng, A.: The ion chemistry and the source of PM_{2.5} aerosol in Beijing, *Atmos. Environ.*, 39, 3771–3784, doi:10.1016/j.atmosenv.2005.03.013, 2005.
- Wang, Y., Zhuang, G., Zhang, X., Huang, K., Xu, C., Tang, A., Chen, J., and Zheng, A.: The ion chemistry, seasonal cycle, and sources of PM_{2.5} and TSP aerosol in Shanghai, *Atmos. Environ.*, 40, 2935–2952, doi:10.1016/j.atmosenv.2005.12.051, 2006.
- 30 Wang, K., Zhang, Y., Nenes, A., and Fountoukis, C.: Implementation of dust emission and chemistry into the Community Multiscale Air Quality modeling system and initial application to an Asian dust storm episode, *Atmos. Chem. Phys.*, 12, 10209–10237, doi:10.5194/acp-12-10209-2012, 2012.



- Wang, H.L., Qiao, L.P., Lou, S.R., Zhou, M., Ding, A.J., Huang, H.Y., Chen, J.M., Wang, Q., Tao, S.K., Chen, C.H., Li, L., and Huang, C.: Chemical composition of PM_{2.5} and meteorological impact among three years in urban Shanghai, China, J. Clean. Prod., 112, 1302–1311, doi:10.1016/j.jclepro.2015.04.099, 2016.
- Wexler, A.S. and Clegg, S. L.: Atmospheric aerosol models for systems including the ions H⁺, NH₄⁺, Na⁺, SO₄²⁻, NO₃⁻, Cl⁻,
5 Br⁻, and H₂O, J. Geophys. Res., 107, 4207, doi:10.1029/2001JD000451, 2002.
- WHO 2006a, Health Risks of Particulate Matter from Long-range Transboundary Air Pollution, E88189. European Centre for Environment and Health, WHO Regional Office for Europe, Denmark, 2006.
- WHO 2006b, WHO Air quality guidelines for particulate matter, ozone, nitrogen dioxide and sulphur dioxide, Global update 2005, Summary of risk assessment, WHO/SDE/PHE/ OEH/06.02, Geneva, Switzerland, 2006.
- 10 Wonaschutz, A., Demattio, A., Wagner, R., Burkart, J., Zikova, N., Vodicka, P., Ludwig, W., Steiner, G., Schwarz, J., and Hitznerberger, R.: Seasonality of new particle formation in Vienna, Austria - Influence of air mass origin and aerosol chemical composition, Atmos. Environ., 118, 118–126, doi:10.1016/j.atmosenv.2015.07.035, 2015.
- Yao, X. H., Lau, A. P. S., Fang, M., Chan, C. K., and Hu, M.: Size distributions and formation of ionic species in atmospheric particulate pollutants in Beijing, China: 1 - inorganic ions, Atmos. Environ., 37, 2991–3000,
15 doi:10.1016/S1352-2310(03)00255-3, 2003.
- Zhang, L. M., Gong, S. L., Padro, J., and Barrie, L.: A size segregated particle dry deposition scheme for an atmospheric aerosol module, Atmos. Environ., 35, 549–560, doi:10.1016/S1352-2310(00)00326-5, 2001.
- Zhang, R., Wang, G., Guo, S., Zamora, M. L., Ying, Q., Lin, Y., Wang, W., Hu, M., and Wang, Y.: Formation of urban fine particulate matter, Chem. Rev., 115, 3803–3855, doi:10.1021/acs.chemrev.5b00067, 2015.
- 20 Zhao, M., Wang, S., Tan, J., Hua, Y., Wu, D., and Hao, J.: Variation of urban atmospheric ammonia pollution and its relation with PM_{2.5} chemical property in winter of Beijing, China, Aerosol Air Qual. Res., 16, 1378–1389, doi:10.4209/aaqr.2015.12.0699, 2016.



Table 1: Basic statistics for the PM₁₀ and PM_{2.5} fractions mass concentrations determined over the investigated period (n = 84 sampling events) in Iasi, north-eastern Romania.

Statistical parameter	PM ₁₀ (µg m ⁻³)			PM _{2.5} (µg m ⁻³)		
	Working day	Weekend	Annual	Working day	Weekend	Annual
Mean	19.25	18.60	18.95	17.31	16.47	16.92
Median	16.05	17.26	16.35	14.01	15.43	14.51
Geomean	16.90	16.91	16.90	14.86	14.83	14.84
Stdev	10.05	8.62	9.35	9.92	8.11	9.07
Min	5.56	7.11	5.56	5.08	6.30	5.08
Max	42.65	44.84	44.84	41.57	43.91	43.91



Table 2: Annual and/or seasonal arithmetic means of the PM₁₀ and PM_{2.5} fraction mass concentrations in Iasi, north-eastern Romania, and other various European sites (mean ± stdev).

Site	Category	Sampling aagl* (m)	Sampling period	PM _{2.5} (µg m ⁻³)	PM ₁₀ (µg m ⁻³)	Reference
Iasi (Romania)	urban	35	2016	16.9±9.1 14.0±7.1 (warm) 21.3±13.0 (cold)	18.9±9.3 16.8±8.3 (warm) 22.6±13.1 (cold)	This work
Iasi (Romania)	urban	25	2007–2008	10.5±11.2	38.3±25.4	Arsene et al., 2011 ^a
Paris (France)	urban background	20	2009–2010	14.8±9.6	–	Bressi et al., 2013
Northern Europe (SE12)	EMEP and 4 regional background sites	–	2012–2013	–	3–8	Alastuey et al., 2016 ^b
North-western Europe (IE321)					10–15 (S); ~ 35 (W)	
Central western Europe (FR09)					10–15 (S); ~ 25 (W)	
Central Europe (DE44)					20–25 (S); 25–30 (W)	
Eastern Europe (SK06,HU02)					10–15 (S); 15–25 (W)	
Eastern Europe (MD13)					~ 25 (S); 25–30 (W)	
South western Europe (ES22)					20–25 (S); 5–10 (W)	
Central southern Europe (IT01)					25–35 (S); 20–25 (W)	
South eastern Europe (GR02)					~ 25 (S); 35–40 (W)	
Thessaloniki (Greece)	urban	7	2011–2012	37.7±15.7	–	Tolis et al., 2015
Thessaloniki (Greece)	urban	3	2011–2012	21.5±8.3 (warm) 33.9±19.3 (cold)	–	Voutsas et al., 2014 ^c
Finokalia (Greece)	remote coastal	~ 5	2004–2006	18.2	30.8	Gerasopoulos et al., 2007
Bologna (Italy)	urban background	courtyard	2005–2006	31.6±21.0	44.5±24.2	Tositti et al., 2014
Venice (Italy)	semi-rural coastal	–	2007–2008	–	22.5±12.9	Masiol et al., 2012
Prague (Czech)	urban	12–25	2004–2005	–	33±13	Schwarz et al., 2008

Note: *sampling altitude above ground level, ^athe total (coarse + fine) and the fine fractions reported (coarse fraction - particles of AED > 1.5 µm and fine fractions - particles of AED < 1.5 µm); ^bS–summer (8 June–12 July 2012), W–winter (11 January–8 February 2013); ^caveraged value of warm and cold seasons data (error propagation method for uncertainty estimation).


 Table 3: Monthly averages of meteorological variables, PM₁₀, PM_{2.5} fractions and of water soluble ions mass concentrations (µg m⁻³) in PM_{2.5} aerosol particles from Iasi, north-eastern Romania. Data are presented as mean±stdev (median).

Month	January	February	March	April	May	June	July	August	September	October	November	December
WS (m/s)	6.41±4.89 (5.60)	7.34±4.74 (6.80)	6.49±4.79 (5.70)	6.41±5.05 (5.60)	5.45±4.44 (4.90)	6.07±4.36 (5.70)	6.28±5.00 (5.40)	5.37±4.72 (4.70)	4.67±3.73 (4.40)	7.17±4.57 (6.80)	5.72±4.92 (4.90)	3.77±3.76 (3.20)
AT (°C)	-1.06±4.71 (-1.42)	5.86±1.98 (6.61)	6.50±3.49 (5.35)	13.65±4.15 (14.48)	15.65±3.25 (15.70)	21.05±4.75 (20.46)	23.27±3.05 (24.58)	21.86±2.13 (21.21)	18.20±5.57 (20.30)	10.03±5.11 (7.86)	7.41±5.86 (6.23)	2.77±2.41 (2.56)
RH (%)	71.27±15.86 (69.57)	68.20±6.97 (68.27)	46.30±27.50 (37.88)	44.43±13.19 (47.27)	50.32±15.88 (47.47)	46.63±16.69 (43.99)	32.95±7.58 (33.97)	37.12±13.14 (35.50)	31.56±14.10 (28.71)	54.30±10.58 (49.64)	69.92±22.10 (72.41)	81.85±13.22 (82.85)
RHD (%)	78.66±3.61 (78.83)	73.54±1.38 (73.01)	73.14±2.34 (73.86)	68.59±2.49 (68.02)	67.37±1.92 (67.30)	64.38±2.54 (64.62)	63.16±1.62 (62.46)	63.88±1.13 (64.21)	65.98±3.16 (64.71)	70.87±3.17 (72.17)	72.61±3.81 (73.27)	75.71±1.73 (75.85)
n*	5	5	8	8	9	8	5	9	7	7	7	6
PM _{2.5}	23.39±11.65 (26.19)	21.30±8.37 (20.65)	16.10±5.31 (14.98)	15.29±8.34 (11.67)	8.98±3.78 (6.88)	11.45±5.61 (9.19)	16.15±11.12 (14.19)	14.00±4.27 (13.70)	17.36±5.60 (17.77)	12.71±4.81 (13.29)	16.93±13.09 (12.04)	30.94±9.51 (24.55)
PM ₁₀	24.25±11.99 (27.86)	22.11±8.50 (21.43)	17.25±5.28 (16.08)	18.22±11.08 (13.18)	12.11±4.43 (14.25)	14.33±6.98 (10.24)	19.05±11.57 (16.00)	16.59±5.52 (16.17)	19.76±6.87 (20.20)	15.13±5.81 (16.49)	18.13±13.58 (13.49)	32.08±9.44 (26.12)
Cl ⁻	0.32±0.15 (0.34)	0.35±0.10 (0.37)	0.14±0.10 (0.10)	0.21±0.16 (0.15)	0.14±0.08 (0.13)	0.14±0.08 (0.14)	0.20±0.11 (0.18)	0.26±0.15 (0.31)	0.19±0.06 (0.18)	0.38±0.24 (0.32)	0.24±0.24 (0.19)	0.55±0.19 (0.64)
NO ₃ ⁻	3.54±1.93 (4.14)	3.21±1.36 (3.14)	2.42±1.09 (2.43)	1.36±0.86 (1.22)	0.47±0.28 (0.41)	0.31±0.17 (0.26)	0.31±0.11 (0.30)	0.41±0.17 (0.33)	0.69±0.41 (0.57)	1.25±0.82 (1.13)	1.88±1.27 (2.12)	3.62±1.10 (4.07)
SO ₄ ²⁻	2.76±1.66 (2.49)	2.58±0.91 (2.50)	2.03±0.71 (2.15)	1.96±0.75 (1.82)	1.70±0.81 (1.53)	2.39±1.31 (2.32)	2.04±0.98 (1.58)	2.22±0.76 (2.04)	2.15±0.84 (2.18)	1.96±1.00 (2.05)	1.17±0.27 (1.16)	2.16±0.69 (2.33)
CH ₃ COO ⁻	0.51±0.31 (0.45)	0.79±0.50 (0.63)	0.30±0.18 (0.29)	0.84±0.36 (0.82)	0.64±0.44 (0.49)	0.58±0.34 (0.57)	0.82±0.53 (0.48)	0.69±0.71 (0.57)	0.70±0.26 (0.60)	0.80±0.28 (0.89)	0.46±0.33 (0.43)	0.59±0.12 (0.54)
HCOO ⁻	0.07±0.05 (0.06)	0.06±0.03 (0.06)	0.09±0.09 (0.05)	0.15±0.20 (0.07)	0.04±0.02 (0.05)	0.05±0.03 (0.04)	0.12±0.11 (0.07)	0.08±0.02 (0.08)	0.09±0.02 (0.10)	0.09±0.04 (0.08)	0.03±0.02 (0.04)	0.07±0.02 (0.07)
C ₂ O ₄ ²⁻	0.08±0.06 (0.08)	0.08±0.04 (0.08)	0.08±0.04 (0.07)	0.08±0.05 (0.08)	0.06±0.04 (0.06)	0.09±0.06 (0.08)	0.12±0.09 (0.10)	0.14±0.05 (0.15)	0.10±0.08 (0.11)	0.06±0.06 (0.04)	0.02±0.02 (0.02)	0.10±0.04 (0.09)
HCO ₃ ⁻	0.39±0.12 (0.43)	0.48±0.24 (0.39)	0.39±0.20 (0.36)	0.65±0.67 (0.39)	0.32±0.17 (0.38)	0.64±0.56 (0.45)	0.51±0.24 (0.56)	2.23±1.95 (1.73)	0.63±0.18 (0.60)	0.25±0.17 (0.24)	0.25±0.34 (0.10)	0.35±0.25 (0.42)
Na ⁺	0.14±0.05 (0.13)	0.17±0.08 (0.16)	0.12±0.08 (0.10)	0.41±0.31 (0.41)	0.19±0.14 (0.10)	0.13±0.05 (0.12)	0.13±0.08 (0.12)	0.18±0.09 (0.17)	0.14±0.09 (0.11)	0.25±0.16 (0.26)	0.12±0.15 (0.08)	0.17±0.09 (0.16)
NH ₄ ⁺ _{total}	2.07±1.08 (2.39)	1.94±0.70 (1.97)	1.48±0.58 (1.57)	0.93±0.25 (0.96)	0.80±0.29 (0.67)	0.90±0.36 (0.86)	0.94±0.40 (0.78)	0.84±0.16 (0.82)	0.97±0.23 (0.92)	1.10±0.48 (1.22)	1.17±0.57 (1.25)	2.09±0.49 (2.37)
K ⁺	0.54±0.25 (0.67)	0.48±0.20 (0.44)	0.27±0.12 (0.25)	0.30±0.13 (0.27)	0.26±0.16 (0.15)	0.28±0.16 (0.24)	0.37±0.21 (0.31)	0.31±0.11 (0.32)	0.45±0.14 (0.48)	0.41±0.13 (0.41)	0.43±0.32 (0.36)	0.71±0.18 (0.65)
Mg ²⁺	0.03±0.01 (0.03)	0.03±0.02 (0.03)	0.02±0.02 (0.01)	0.04±0.04 (0.02)	0.01±0.00 (0.01)	0.02±0.02 (0.02)	0.02±0.00 (0.01)	0.05±0.04 (0.03)	0.02±0.01 (0.02)	0.03±0.02 (0.03)	0.01±0.01 (0.01)	0.03±0.01 (0.03)
Ca ²⁺	0.21±0.07 (0.22)	0.27±0.08 (0.26)	0.22±0.07 (0.19)	0.28±0.24 (0.21)	0.15±0.05 (0.17)	0.30±0.25 (0.22)	0.25±0.12 (0.23)	0.92±0.84 (0.65)	0.30±0.08 (0.31)	0.15±0.08 (0.15)	0.16±0.17 (0.10)	0.20±0.12 (0.20)
pH _{total}	4.20±2.32 (2.88)	4.17±2.53 (3.27)	3.94±2.81 (2.51)	3.88±2.97 (1.80)	3.95±3.10 (2.82)	4.14±2.92 (2.27)	4.58±2.87 (4.26)	5.06±2.73 (7.14)	4.24±3.19 (3.55)	4.25±2.75 (3.60)	3.86±2.55 (2.54)	4.12±2.16 (2.87)

Note: *n represent the number of aerosol sample events collected each month


 Table 4: Correlation matrix (Pearson coefficients) for major ionic species (Cl^- , NO_3^- , SO_4^{2-} , CH_3COO^- , HCOO^- , $\text{C}_2\text{O}_4^{2-}$, HCO_3^- , Na^+ , $\text{NH}_4^+(\text{total})$, K^+ , Mg^{2+} , Ca^{2+}) in fine aerosol particles from Iasi, north-eastern Romania, both for cold (a) and warm (b) seasons.

(a)												
$\text{PM}_{2.5}$ (cold)	Cl^-	NO_3^-	SO_4^{2-}	CH_3COO^-	HCOO^-	$\text{C}_2\text{O}_4^{2-}$	HCO_3^-	Na^+	$\text{NH}_4^+(\text{total})$	K^+	Mg^{2+}	Ca^{2+}
Cl^-	1.00	0.75	0.59	0.56	0.57	0.71	0.22	0.49	0.73	0.80	0.35	0.04
NO_3^-		1.00	0.91	0.37	0.74	0.87	0.13	0.04	0.98	0.85	0.00	0.06
SO_4^{2-}			1.00	0.43	0.72	0.87	0.05	0.02	0.96	0.72	0.07	0.11
CH_3COO^-				1.00	0.56	0.63	0.13	0.17	0.45	0.47	0.01	0.03
HCOO^-					1.00	0.85	0.04	0.01	0.76	0.65	0.12	0.09
$\text{C}_2\text{O}_4^{2-}$						1.00	0.23	0.08	0.89	0.76	0.16	0.17
HCO_3^-							1.00	0.56	0.17	0.05	0.76	0.98
Na^+								1.00	0.03	0.06	0.83	0.50
$\text{NH}_4^+(\text{total})$									1.00	0.82	0.08	0.12
K^+										1.00	0.08	0.09
Mg^{2+}											1.00	0.66
Ca^{2+}												1.00
(b)												
$\text{PM}_{2.5}$ (warm)	Cl^-	NO_3^-	SO_4^{2-}	CH_3COO^-	HCOO^-	$\text{C}_2\text{O}_4^{2-}$	HCO_3^-	Na^+	$\text{NH}_4^+(\text{total})$	K^+	Mg^{2+}	Ca^{2+}
Cl^-	1.00	0.57	0.10	0.81	0.37	0.08	0.81	0.87	0.02	0.76	0.83	0.63
NO_3^-		1.00	0.34	0.02	0.14	0.17	0.63	0.71	0.23	0.08	0.86	0.39
SO_4^{2-}			1.00	0.01	0.66	0.76	0.17	0.05	0.97	0.43	0.03	0.01
CH_3COO^-				1.00	0.32	0.11	0.30	0.07	0.11	0.55	0.05	0.08
HCOO^-					1.00	0.58	0.32	0.01	0.66	0.59	0.02	0.01
$\text{C}_2\text{O}_4^{2-}$						1.00	0.58	0.04	0.71	0.46	0.01	0.15
HCO_3^-							1.00	0.45	0.06	0.13	0.12	0.99
Na^+								1.00	0.11	0.19	0.76	0.38
$\text{NH}_4^+(\text{total})$									1.00	0.49	0.12	0.12
K^+										1.00	0.02	0.03
Mg^{2+}											1.00	0.81
Ca^{2+}												1.00



Figure captions

Figure 1: Sectors contributions identified from classification of 2-day back trajectories of air masses ending at Iasi and representative backward trajectories of long and short range transport, Black Sea influence and African dust (shown trajectories correspond to sampling events).

Figure 2: Patterns of the monthly arithmetic mean concentrations and standard deviations in the PM_{10} , $PM_{2.5}$ and $PM_{2.5}/PM_{10}$ variables at Iasi, north-eastern Romania.

Figure 3: Size distribution histograms of aerosol particles mass concentration gravimetrically determined over both the cold and warm seasons.

Figure 4: Distribution of the aerosol pH predicted by ISORROPIA-II (forward mode) vs. the ion balance (a), sensitivity of aerosol pH predicted with the model to small changes in the input aerosol NH_4^+ concentration (b) and bar chart distribution in aerosol pH over the warm and cold season both for NH_4^+ derived from raw IC data (c) and NH_4^+ (total) (d).

Figure 5: Size distribution of averaged aerosol mass, NO_3^- , SO_4^{2-} and NH_4^+ concentrations over cold (a) and warm (b) seasons accompanied by the size distribution of ISORROPIA-II estimated pH and H^+ mass concentration over both the cold (c) and the warm (d) seasons.

Figure 6: Seasonal variations for selected water-soluble ionic components in the $PM_{2.5}$ fraction (a-h) and variation of the mixed layer depth at the investigated site (i). The inset distribution presented within NO_3^- seasonal variation reflects the contribution of the coarse fraction over the warm seasons. The horizontal black line represents the mean, the horizontal colored line – the median, the box – the 25–75% percentiles, the length of the whiskers plot – the 10 and 90% of observed concentrations, circles – outliers).

Figure 7: Regression analysis of the $[NH_4^+]$ vs. $(2 \times [SO_4^{2-}])$ (a, b), $[NH_4^+]$ vs. $([NO_3^-] + 2 \times [SO_4^{2-}])$ (c,d) and $[NH_4^+]$ vs. $([Cl^-] + [NO_3^-] + 2 \times [SO_4^{2-}])$ (e,f) dependences specific for $PM_{2.5}$ particles.

Figure 8: The relative contributions, as monthly-based averages, of identified and quantified water soluble ions to total detected components in the 0.0276–0.0945 μm (a), 0.155–0.612 μm (b), 0.946–2.39 μm (c) and 3.99–9.94 μm (d) size range grouped fractions.

Figure 9: Size distributions of seasonal averaged mass concentrations for Cl^- , NO_3^- , SO_4^{2-} , NH_4^+ (a,b) and K^+ , Na^+ , Mg^{2+} , Ca^{2+} (c,d) ions in atmospheric aerosols from Iasi, both during the cold and, respectively, the warm seasons.

Figure 10: Evidences of long range transport contributions from Saharan dust within the size distribution of particulate Na^+ , Ca^{2+} , Mg^{2+} , Cl^- ions and aerosol mass (a) and of air masses buoyancy phenomena within the size distribution of particulate NH_4^+ , NO_3^- , SO_4^{2-} , Mg^{2+} ions and aerosol mass (b).

Figure 1

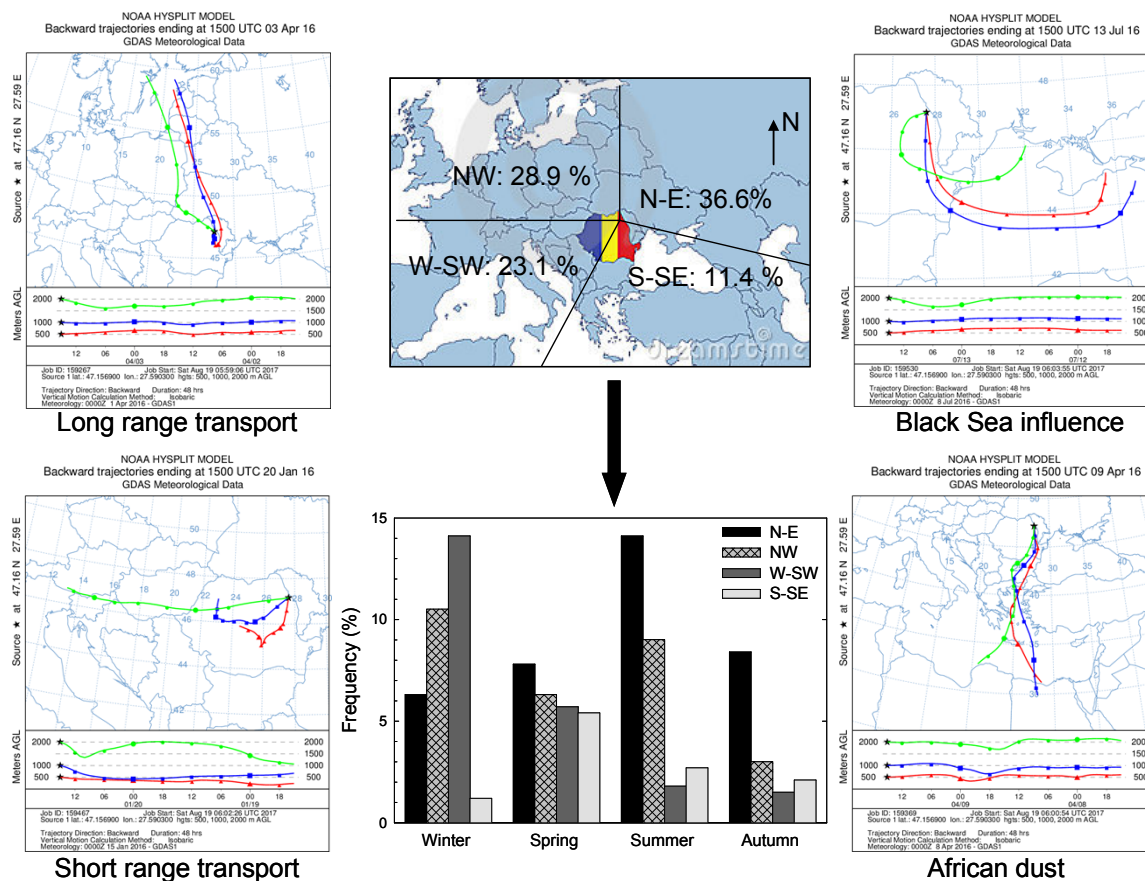




Figure 2

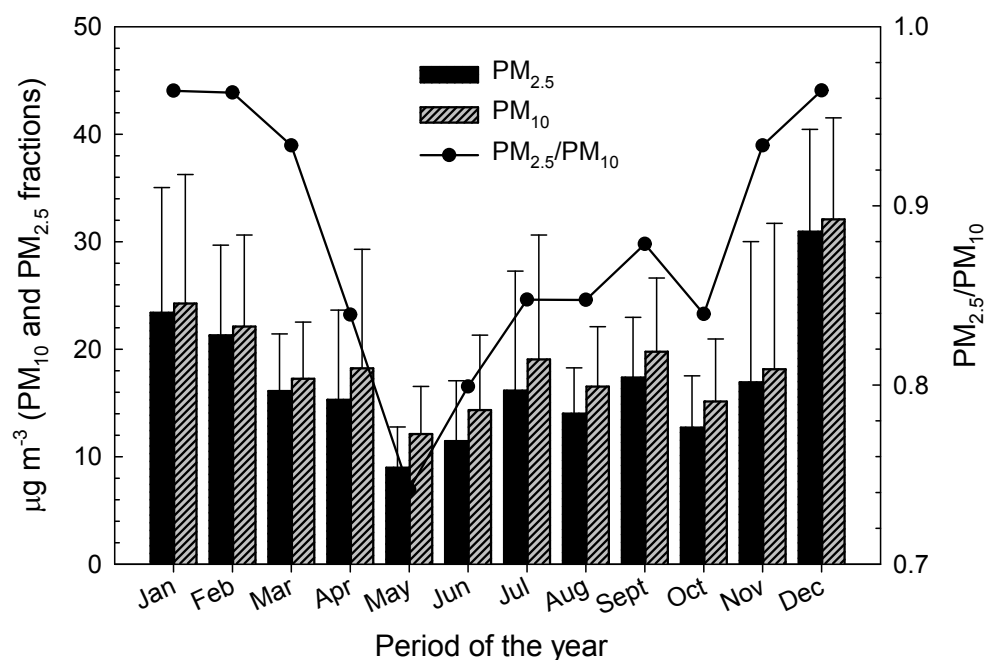




Figure 3

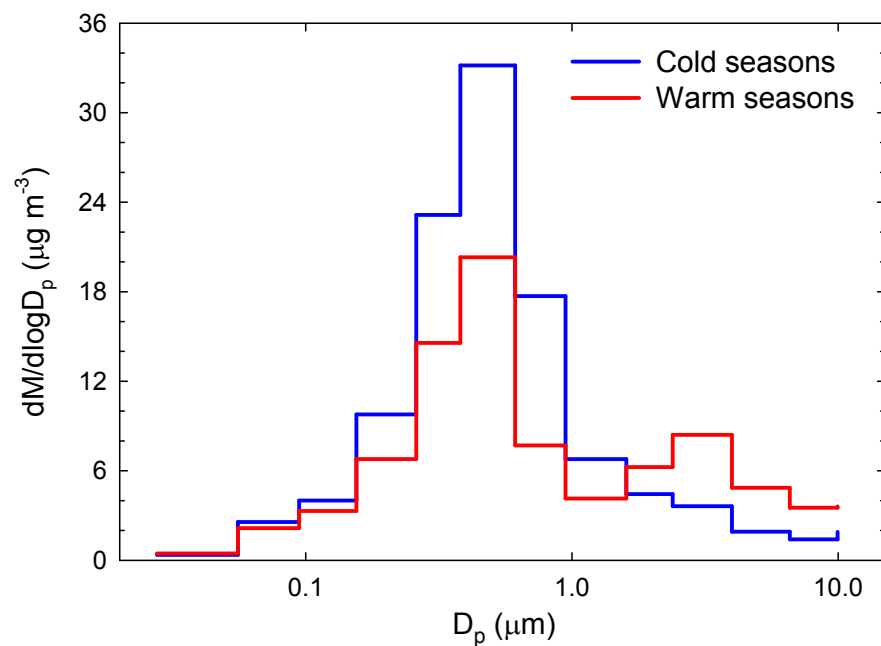




Figure 4

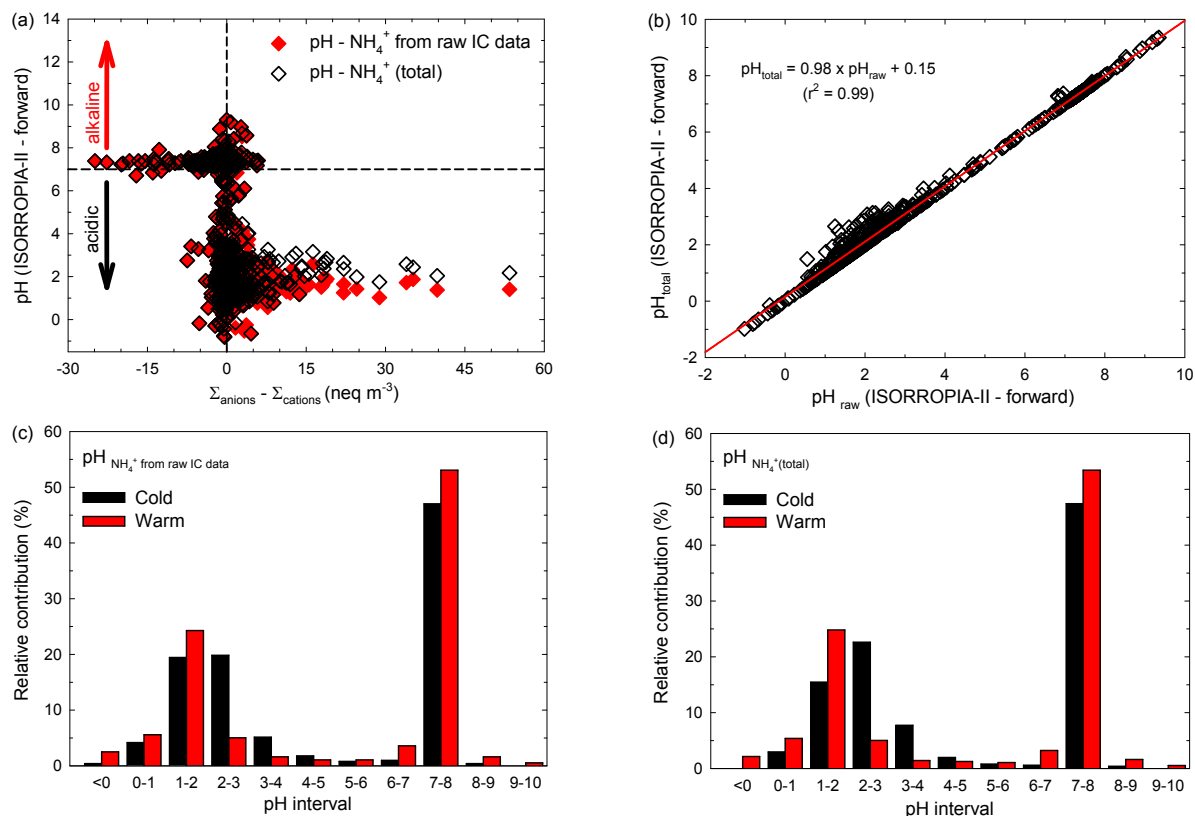




Figure 5

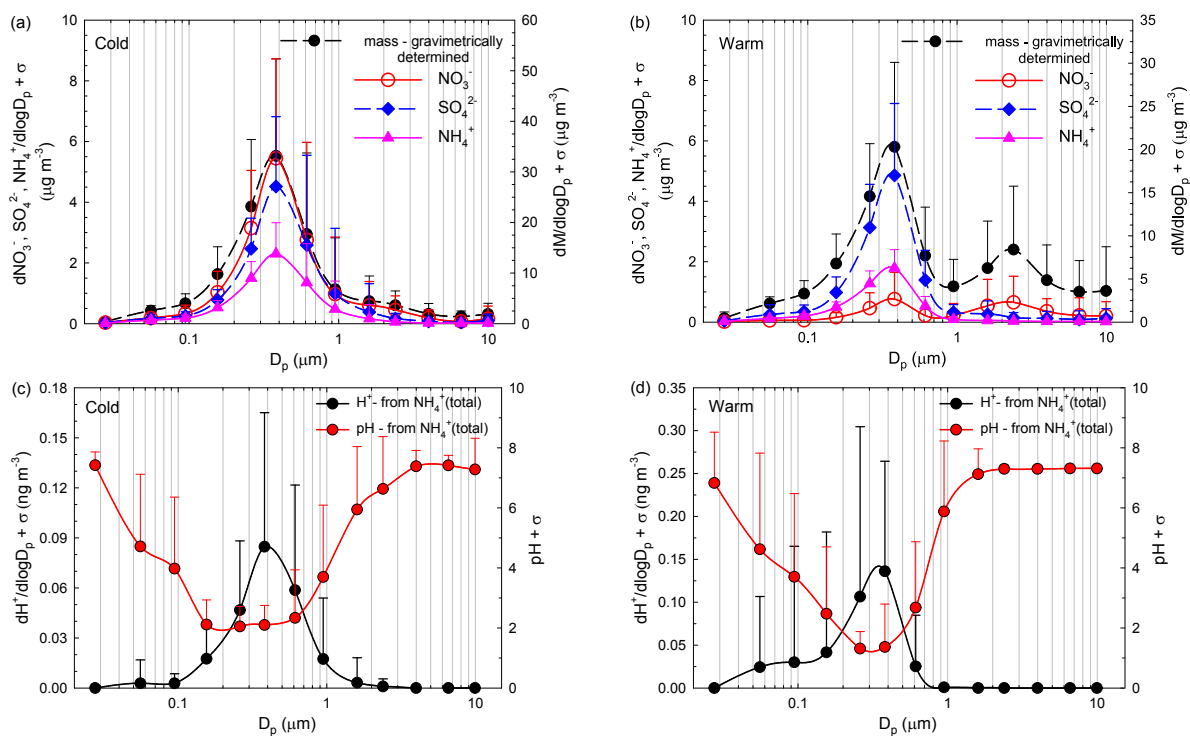




Figure 6

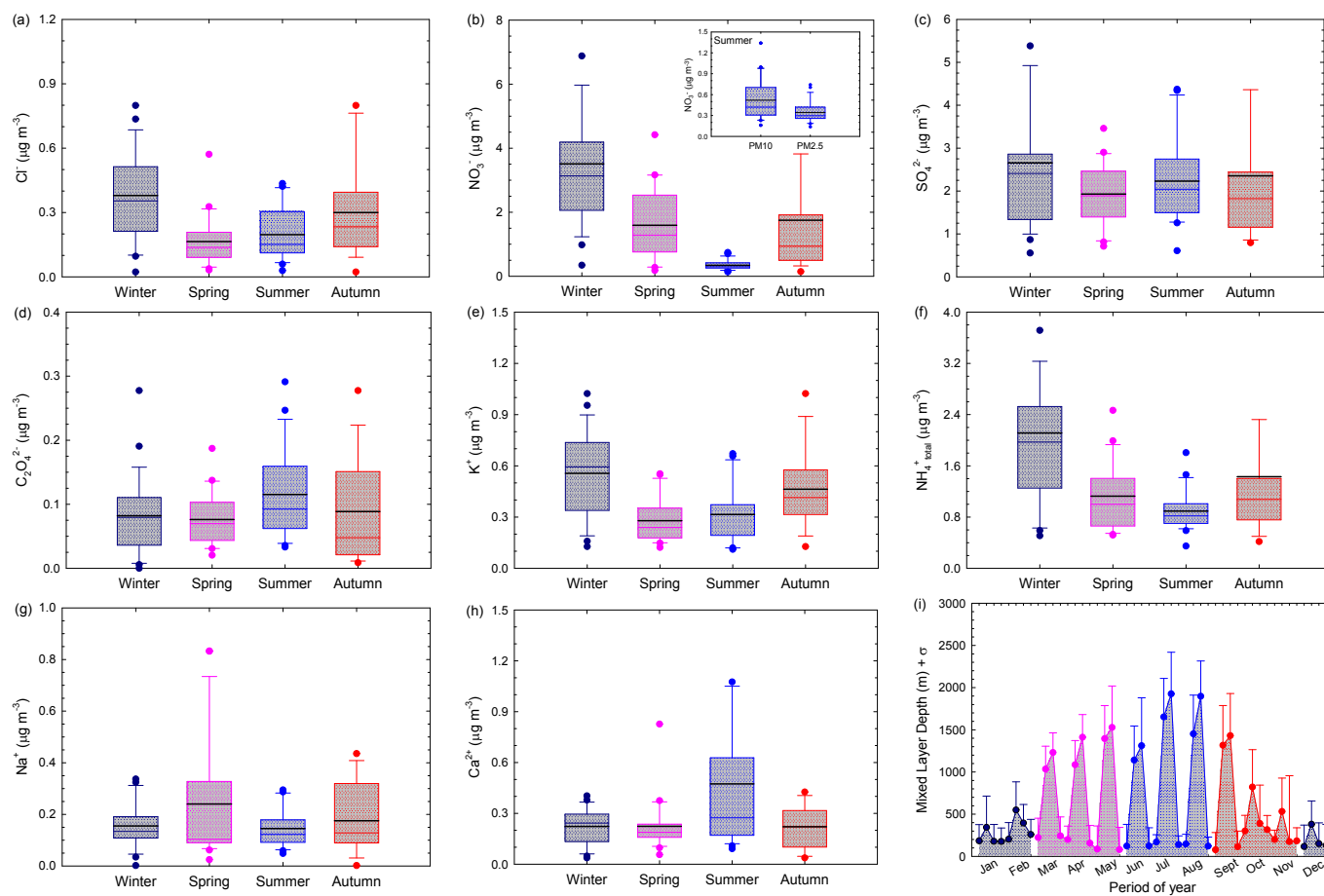




Figure 7

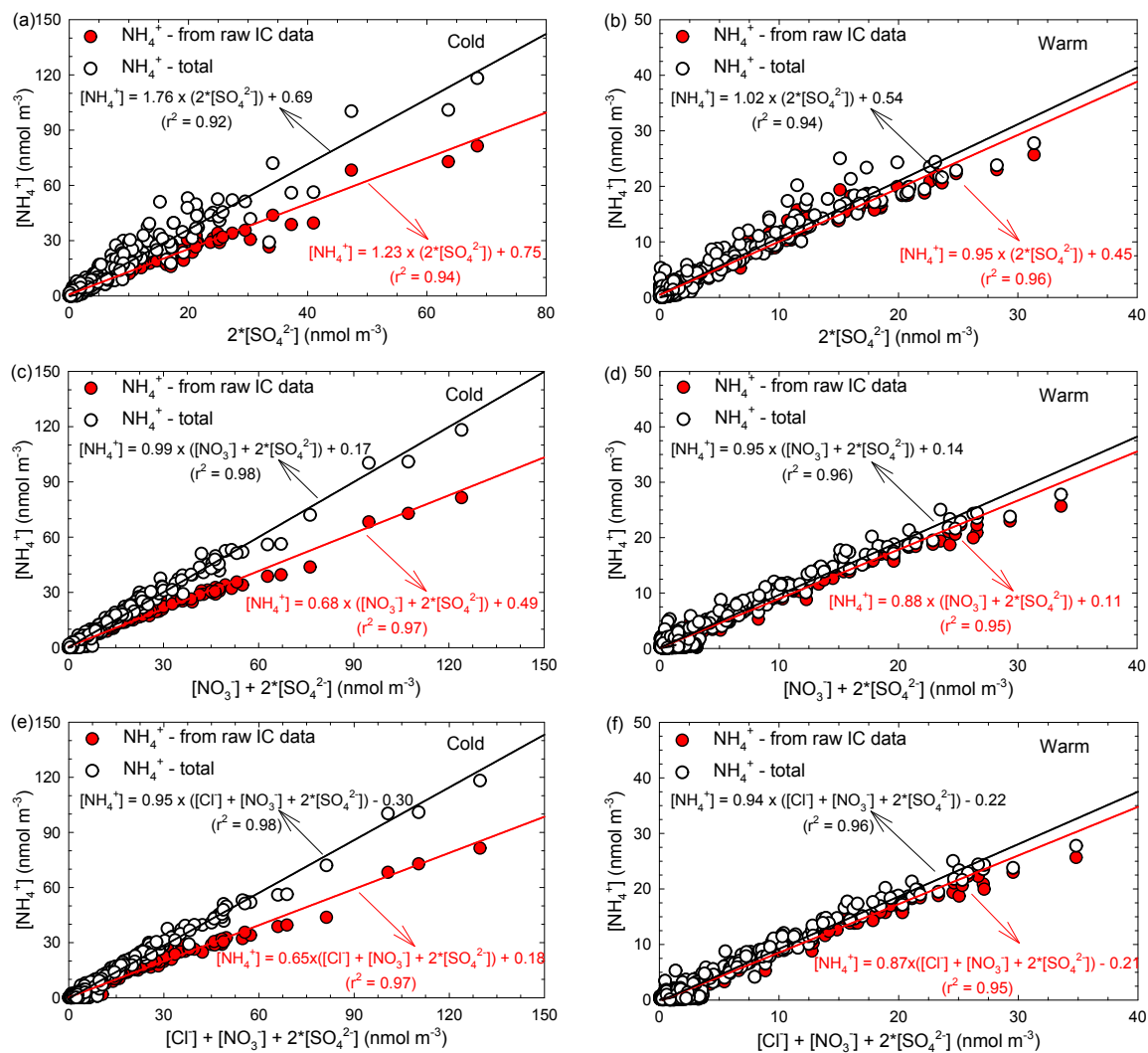




Figure 8

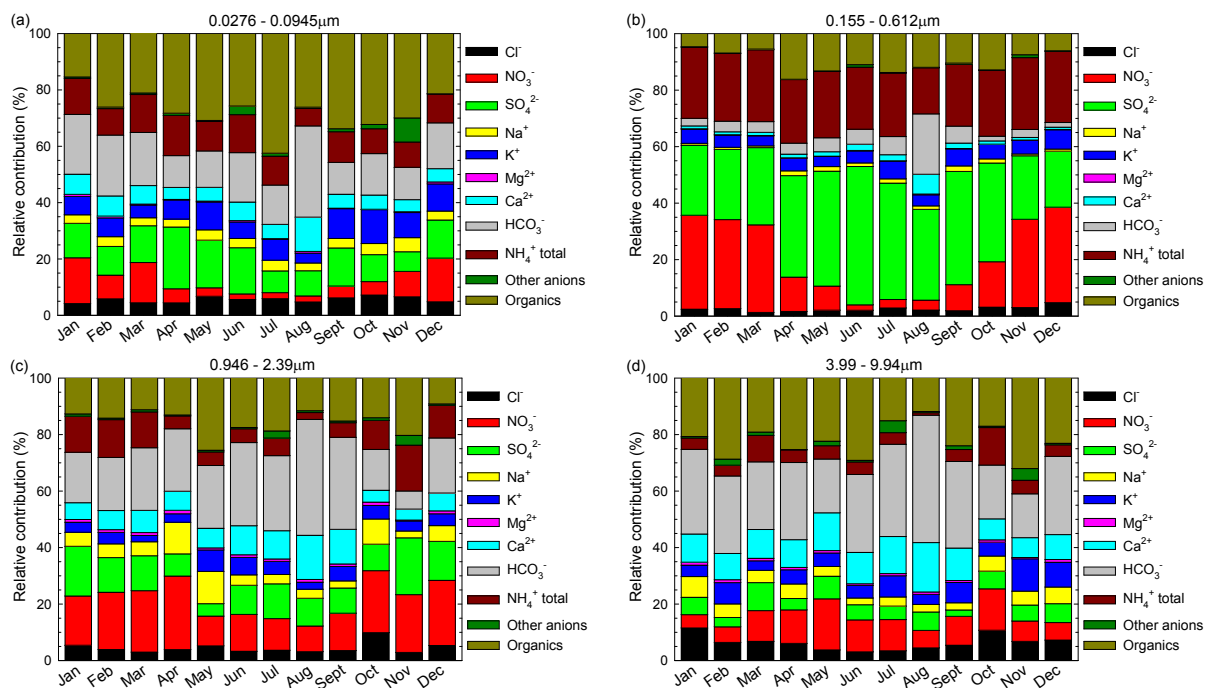




Figure 9

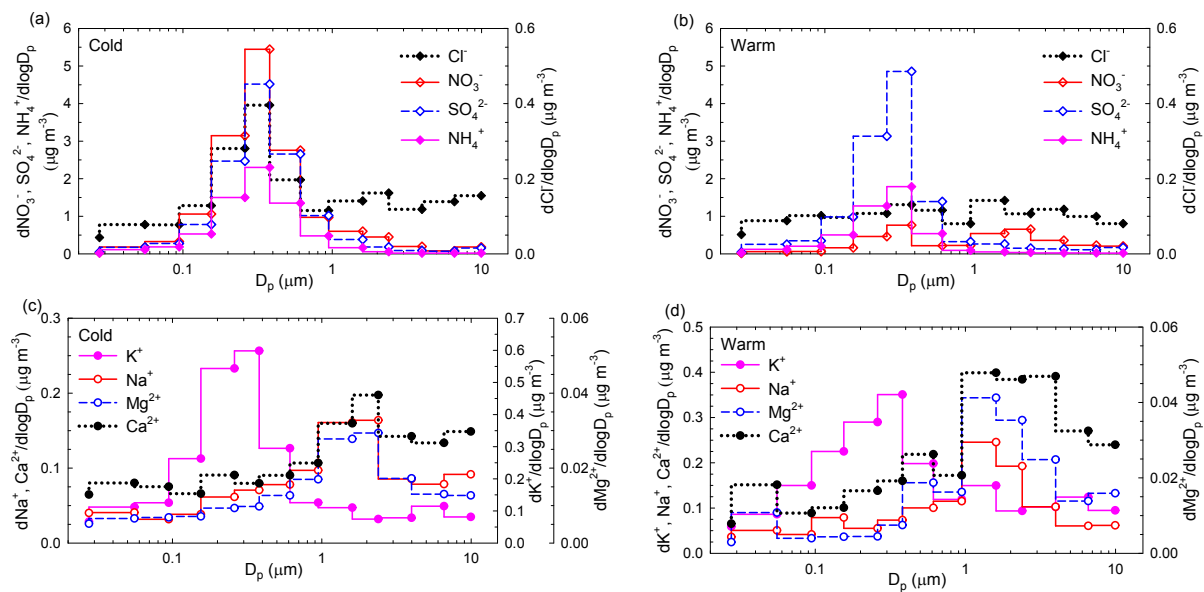




Figure 10

